DEPARTMENT OF DEFENCE

DSTO

Optoelectronics Division

TECHNICAL REPORT
SRL-0109-TR

EVALUATION OF A SINGLE STAGE OF THE LADS FILTER

by

R.S. Seymour, S. Kees, J. Staromlynska, J. Richards and P. Wilson

SURVEILLANCE RESEARCH LABORATORY

AR-008-107

DSTO AUSTRALIA

SURVEILLANCE RESEARCH LABORATORY

Optoelectronics Division

TECHNICAL REPORT
SRL-0109-TR

EVALUATION OF A SINGLE STAGE OF THE LADS FILTER

by

R.S. Seymour, S. Rees, J. Staromlynska, J. Richards and P. Wilson

SUMMARY

A tunable, large aperture, wide angle, narrowband filter, centred at 532 nm, has been developed to improve the signal to noise in the Laser Airborne Depth Sounder. Several new concepts have been included in the design.

NOV 92

APPROVED FOR PUBLIC RELEASE

POSTAL ADDRESS: Director, Surveillance Research Laboratory, PO Box 1500, Salisbury, South Australia, 5108.

CONTENTS

FIGURES

TABLES

THIS PAGE BLANK

EXECUTIVE SUMMARY

A narrowband wide angle filter has been proprosed to improve the ability of the LADS system to detect laser light reflected from the sea bottom in the presence of ambient daylight. Modelling of the performance of complete filters and an experimental evaluation of a single stage have allowed a construction proposal to be made for the narrowband filter. This report gives a detailed discussion of the various component choices and design tradeoffs. A birefringent filter is considered to be the most appropriate filter type to achieve the required performance. Such a filter is constructed from a number of discrete stages, each separated by a polariser. The main birefringent components of each stage are made from single crystal lithium niobate. For the filter to achieve the required field of view, all six stages are of a wide field type. The wide field stages have an additional component which is used as a half wave plate. Liquid crystal variable retarders are used in each of the stages to compensate for changes in the filter pass wavelength due to temperature fluctuations. In addition, a dielectric filter is necessary to suppress ambient light outside the free spectral range of the birefringent filter. The bandwidth of the birefringent filter is determined by the thickest element and the free spectral range by the number of stages. Numerical modelling shows the optimum bandwidth to be **0.1 nm** which corresponds to a thickness of the thickest element of **9.6 mm**. The net effect of the transmittance of each component in the filter determines the overall signal available to the receiver detector. The normal incidence transmittance for the six stage filter is **30%** at the laser wavelength. This compares to **25%** for an existing dielectric filter used by LADS. A comparison of the proposed birefringent filter and the dielectric filter currently used by LADS, which also takes account of field of view and bandwidth, indicates that the ratio of signal to ambient will be improved by a factor of approximately **20** for daytime operation in clear water. The length of the proposed filter, not including its housing, is **192 mm**, assuming a 1 mm air gap between each of the **29** components.

Conclusions from this study are: that a filter can be made that will significantly improve the daytime performance of the LADS system and; that the remaining scientific risk in the construction of the proposed filter is small.

THIS PAGE BLANK

1 INTRODUCTION

The performance of the Laser Airborne Depth Sounder (LADS) system depends on its ability to discriminate between the laser wavelength reflected from the sea bottom and the ambient light. A filter is being developed to limit the ambient light so that greater depths can be recorded in clear water during daytime with ideally only the deepest water requiring charting at night. The filter should have a narrow passband at the laser operating wavelength (532 nm), a wide field of view (± 8.5°), good sideband rejection, and a large aperture (50 mm). This specification is further discussed in section 3 of this report.

A design concept based on a multistage Lyot filter [1], has been developed and is described in section 3. The performance of such a device depends ultimately on the performance of the individual components in each stage. These include polarisers, liquid crystal variable retarders, birefringent crystals and broadband half wave plates. Subsequent sections of this report deal with measurements on such components acquired from various commercial sources. The effect of imperfections in the components on filter operation is assessed with the aid of a numerical model based on a complete theoretical description of the optics of anisotropic media. The detail of this model is reported elsewhere, [2]. Simpler treatments of the optics can be used to estimate the cumulative effects of imperfect components to give a guide to the tolerances that need to be placed on the various components. Some results from a model using this simpler theory are reported in section 6. An assessment of closed loop tuning of a single stage of the filter, which is used to ensure that the transmission peak is optimised irrespective of temperature induced changes or slight shifts in laser wavelength, is presented in section 7. A complete single stage of the filter has been experimentally assessed in section 5 and finally, recommendations are made with respect to future construction of the full filter.

2 FILTER SPECIFICATIONS

2.1 Laser wavelength

The LADS laser wavelength, its linewidth and temperature variation have been measured using a scanning Fabry-Perot wavemeter. The results showed a line width of 0.02 nm centred at 531.96 nm at low laser power, and shifting to 531.99 nm at high laser power. These results suggest a minimum desirable linewidth for a filter of 0.05 nm. Initially a value of 0.15 nm was chosen to enable adequate field of view (FoV) and to keep the length of the filter construction below a limit set by retrofit considerations, however subsequent considerations (see sections 3.3.1 and 6.) altered this to 0.06 nm.

2.2 Field of View

The return signal to the LADS receiver has a large angular spread due to scatter on its passage through the seawater. To increase the maximum depth measurable it is desired to optimise collection of the reflected photons. The receiver telescope collects light to a half angle of 20 mrad which corresponds to a field of view of 8.5° at the focal plane. A suitable wide angle filter should maintain its pass band centred at the laser wavelength for angles of incidence to 8.5° giving increased signal (over low angle filters) without associated increase in collection of ambient light (noise).

2.3 Signal to Noise

The signal to noise ratio (SNR) of the return light is a crucial parameter determining the depth performance of the LADS system. (Noise in the context of this report does not refer to random or statistical noise present due to the detector or its associated electronics or that arising from backscatter in the water column but is equal to the level of ambient light leakage through the filter). The effect of the filter on the SNR is the integral of the filter transmittance $T(\lambda)$ in the laser passband $\Delta\lambda_L$ multiplied by the collected signal flux $I_s(\lambda)$ compared to the integral of the filter transmittance multiplied by the ambient light or noise flux $I_N(\lambda)$

$$snr = \frac{\int^{\Delta\lambda_L} T(\lambda)\, I_s(\lambda)\, d\lambda}{\int^{\Delta\lambda_R} T(\lambda)\, I_N(\lambda)\, d\lambda}$$

This can be approximated by (see Figure 1),

$$snr = \frac{T(\lambda_L)\, \Delta\lambda_L\, I_s}{T\, I_N\, \Delta\lambda_R}$$

where I_s is the collected signal flux at the laser wavelength, and $\Delta\lambda_R$ is the effective total bandwidth of the receiver without the filter. T is the average filter transmittance over the receiver bandwidth and is a measure involving the bandwidth, peak transmittance and sideband transmittance of the filter spectral response. In the simplest case

$$\Delta\lambda_R\, T = T(\lambda_L)\ \Delta\lambda_F + T_N\, \Delta\lambda_R$$

where $\Delta\lambda_F$ is the filter bandwidth and T_N is an average sideband transmittance. Comparison of two filters leads to

$$S = \frac{snr_1}{snr_2} = \frac{T_1(\lambda_L)\, I_{s_1}\, (T_2(\lambda_L)\Delta\lambda_{F_1} + T_N\Delta\lambda_R)}{T_2(\lambda_L)\, I_{s_2}\, (T_1(\lambda_L)\Delta\lambda_{F_1} + T_N\Delta\lambda_R)} \cdot \frac{I_{N_2}}{I_{N_1}}$$

S is directly proportional to the ratio of filter transmittance at the laser wavelength and to the ratio of collected signal fluxes (which depend on filter FoV considerations) and inversely proportional to the averaged filter transmittances. Although these expressions do not contain details of filter spectral transmittance they are sufficient to illustrate the relative importance of the variables involved. As an example, consider a filter with a bandwidth of 1 nm and transmittance at λ_L of 25% designed to transmit over the 8.5° FoV of the receiver telescope. If an alternate filter design has the same FoV but with a bandwidth of 0.06 nm then an improvement in SNR by a factor of 10 can be expected for the same transmittance and a value for $T_N\, \Delta\lambda_F$ of 0.04 (equivalent

transmittance of 0.1% over 40 nm). Similarly an estimate of the performance of the 0.06 nm filter for operation in daylight compared to the operation at night without a filter can be made. In this case

$$S = T_1(\lambda_1) \cdot \frac{I_{N_2}}{I_{N_1}} \cdot 1000$$

here I_{N_2} and I_{N_1} are the background night and daytime fluxes. The factor 1000 is an estimate of the reciprocal of T_1, the average filter transmittance over the receiver bandwidth. Values of I_{N_2}/I_{N_1} could range from 10^{-8} when comparing a bright sunlit day to an overcast moonless night, to 10^{-4} for an overcast day to moonlit night comparison [3]. The worst case comparison gives $S=10^{-5}$ and best case $S=10^{-1}$. In section 6, further comparisons of performance of various filters are made obtained using detailed spectral transmittances.

2.4 Free Spectral Range

Many filter concepts, and in particular the birefringent filters discussed in the next section, have a spectral transmittance consisting of a series of narrow peaks, with the separation of peaks called the free spectral range (FSR). A secondary filter is required to eliminate all other peaks of the primary filter except the one centred at the laser wavelength. The secondary filter needs to have a passband of high transmittance over the full field of view required. The specification for the FSR of the primary filter is determined by the performance of the secondary filter. A convenient choice for the secondary filter is a multilayer thin film dielectric stack (see section 4) and from previous experience in the design and construction of such devices a value of 4 nm for the FSR of the primary filter was specified. Comparison of 8 nm and 4 nm systems are described in section 6.

3 FILTER CONCEPT

3.1 Birefringent Filters

Birefringent filters have a narrowband transmittance and a wide angle response [4,5]. Such filters are based on the wavelength variation of phase delays introduced between orthogonal polarisation components of light by the use of suitably oriented birefringent elements, usually single crystal plates. The simplest example is a birefringent crystal between parallel linear polarisers. The crystal is oriented with its optic axis in the plane of the plate and rotated by 45° with respect to the pass plane of the polarisers. The relative phase shift or retardance, at a particular wavelength λ, between the two polarisation components is given by

$$\Gamma(\lambda) = \frac{2\pi \Delta n d}{\lambda}$$

where Δn is the material birefringence and d is the thickness. If Δn has a strong dependence on wavelength then it can dominate the wavelength dependence of Γ and this can be utilised in "dispersive birefringence" filters [4]. The intensity transmitted through the final polariser is given by

$$I(\lambda) = I_0 \cos^2 \frac{\Gamma(\lambda)}{2}$$

where I_0 is the incident intensity. Various combinations of birefringent elements and polarisers can be used to tailor a filter's spectral response, with the two most common types being the Lyot and Solc [5].

Two variations of a Lyot design have been considered for the LADS application, one based on highly dispersive birefringent material and the other on low dispersion material. A Lyot filter consists of a series of stages separated by polarisers. The thicknesses of the birefringent material in the N stages are in the ratio 2^{N-1}:.... 2:1. The total transmittance of the structure is the product of $\cos^2$ terms and has maxima at wavelengths given by

$$\frac{\Delta n d}{\lambda} = M$$

where M is an integer and d is the thickness of the thinnest plate. Other parameters of interest for the filter are bandwidth, free spectral range and field of view. Expressions for these [4] depend on the dispersion of the birefringence α given by

$$\alpha = \frac{d(\Delta n)}{d\lambda}$$

bandwidth:

$$\Delta\lambda_{1/2} = \frac{.886\,\lambda}{2^N d(\alpha - \frac{\Delta n}{\lambda})} = \begin{cases} \dfrac{.886\lambda}{2^N d\alpha} & \textit{dispersive} \\ \dfrac{.886\lambda^2}{2^N d\Delta n} & \textit{non-dispersive} \end{cases}$$

free spectral range:-

$$\Delta\lambda_F = \frac{\lambda}{d(\alpha - \frac{\Delta n}{\lambda})} = \begin{array}{ll} \frac{\lambda}{\alpha d} & \textit{dispersive} \\ \frac{\lambda^2}{\Delta n d} & \textit{non-dispersive} \end{array}$$

field of view:-

$$\theta^2 = \frac{n^2(\alpha - \frac{\Delta n}{\lambda})\Delta\lambda_{1/2}}{\Delta n} = \begin{array}{ll} \frac{n^2\alpha\Delta\lambda_{1/2}}{\Delta n} & \textit{dispersive} \\ \frac{n^2\Delta\lambda_{1/2}}{\lambda} & \textit{non-dispersive} \end{array}$$

where n is an average value of refractive index. The field of view can be greatly increased by the use of Lyot's split elements [5]. These consist of a plate of thickness d split into two of thickness d/2 with the second rotated to have its optic axis at 90° to the first. The two plates are separated by a broadband half wave plate and the combination has increased field of view given by the expressions [4]

$$\theta^2 = \left(\frac{2n}{\Delta n}\right) \cdot \frac{n^2\alpha\Delta\lambda_{1/2}}{\Delta n} \quad \textit{dispersive}$$

$$\textit{or} = \left(\frac{2n}{\Delta n}\right) \cdot \frac{n^2\Delta\lambda_{1/2}}{\lambda} \quad \textit{non-dispersive}$$

Some preliminary consideration was given to Solc filters in an effort to meet the LADS requirement. A Solc filter is made up of a series of n birefringent plates of the same thickness but oriented at different angles and usually in a sequence such as ρ, 3ρ, 5ρ.....$(2n-1)\rho$ where $\rho = 45°/n$. The bandwidth is determined by the number of plates and the FSR by the plate thickness. A principal advantage of Solc filters is that only two polarisers are required, one at the entrance and one at the exit, so that the high transmittance loss due to polarisers (see section 4.3) is minimised. Simple Solc filters are described by similar expressions to those above for the Lyot filters. A disadvantage of the simple Solc is the large number of elements required, typically double the number in a similarly performing Lyot filter. Additionally, the simple Solc has increased sideband transmittance over the Lyot design. Modifications to the basic Solc have been considered by Title and Rosenberg [6] who have demonstrated the versatility of their approach to reducing both the number of elements and the sideband transmittance. However, we have been unable to find a technique suitable for the design of this type of filter which incorporates field of view considerations.

Although the model in [2] allows calculation of field of view for a given design, we know of no intuitive way to produce a Solc design for a given bandwidth, finesse and field of view.

3.2 Materials Selection

One of the main purposes of the assessment of a single filter stage was to determine the relative merits of dispersive and nondispersive birefringent filters. For a nondispersive filter the major materials requirements are a moderately high birefringence, high material uniformity over a 50 mm aperture, chemical and mechanical robustness and ease of fabrication. To achieve a 0.15 nm bandwidth at 532 nm, a material such as lithium niobate with birefringence of 0.09 would need to have a thickness of d = 9.4578 mm. Quartz, which would otherwise be very suitable, would need to be a factor of 10 thicker, whereas calcite would be half as thick but large size, uniform material is not available. Other medium to high birefringence materials are not acceptable either because of a lack of robustness or unavailability in the required size. Lithium niobate, $LiNbO_3$, is an artificially grown crystal available in large sizes. Considerable experience in polishing this material exists in Australia in Applied Physics Division of CSIRO [7]. $LiNbO_3$ was therefore chosen for assessment of the nondispersive Lyot filter concept.

Less choice was available for a dispersive birefringent material and following Yeh, cadmium sulphide, CdS, was chosen for study because of its large value of α, robustness and availability.

3.3 Filter Structure

3.3.1 Nondispersive filter

The bandwidth and free spectral range specifications determine the Lyot filter design. For example, for a 0.15 nm bandwidth and FSR of 5 nm, a five stage filter is required. With $LiNbO_3$ as the birefringent material (Δn=0.09 at 532 nm) the thickest stage needs to be 9.4578 mm and order M=1600 to be centred at 532 nm. The thinnest stage is 0.5912 mm or order M = 100. The field of view requirement of 8.5° can be satisfied by individual stages if the four thickest stages are split elements. Fields of view calculated for each stage using the previously given expressions are summarised in Table 1. Also included is the FoV for a M = 3200 (18.9156 mm) which would have a bandwidth of 0.75Å. These calculations give an indication of the coarse features (number of stages, thickness of elements) of a filter design to meet the requirements for the LADS application. Refinement of this design can be achieved with modelling described in section 6.

Table 1. Field of view calculations for $LiNbO_3$ at 532 nm

Stage	M	FoV	FoV (split)	%T at 8.5°
1	1600	2.17°	15.42°	96
2	800	3.01°	21.81°	98
3	400	4.34°	32.84°	99
4	200	6.13°	43.62°	99
5	100	10.9°	65.68°	70*
0	3200	1.53°	10.9°	84

*indicates value for non split element

Note that the FoV expression given by Yeh [4] defines FoV as half the angle to the first minimum when transmittance is plotted as a function of incident angle. At this point the transmittance will be 50% of maximum. To ensure greater than 70% transmittance at 8.5° would require a FoV of 11° suggesting that it may be necessary to also split the fifth stage element. The effect on overall filter performance of various combinations of split elements including sideband implications, will be examined in greater detail with the model described in section 6.

3.3.2 Dispersive filter

To accurately model a dispersive birefringent filter based on CdS it is necessary to know the variation of the refractive indices with wavelength around 532 nm. Accurate experimental data was not available, however polynomial expressions have been fitted to data at wavelengths of 525 nm (the isoindex point), 532 nm, 550 nm and 589 nm. The fitted expressions were

$$n_o(\lambda) = a_o + b_o \lambda^2 + c_o \lambda^{-2} + d_o \lambda^{-4}$$

and

$$n_e(\lambda) = a_e + b_e \lambda^2 + c_e \lambda^{-2} + d_e \lambda^{-4}$$

The data used and the values obtained for the coefficients of the polynomials are summarised in Table 2.

Table 2. Data and polynomial coefficients for CdS refractive index

	.525μm	.532μm	.550μm	.589μm	a	b	c	d
n_o	2.65	2.625	2.580	2.509	136.06	-139.0	-40.97	4.40
n_e	2.65	2.633	2.593	2.525	-4.03	10.14	2.83	-0.15

The value of α at 532 nm is 0.81 x 10^{-3} nm^{-1} from the calculated expressions. This value of α gives a bandwidth of 0.146 nm for a 2 mm thickness of CdS as the thickest slice of a multistage filter. The FoV for this thickest stage is 18° without the use of a split element. If the total five stage structure is made of CdS, the FSR will be 5.3 nm but the thinnest stage is only 125 microns thick.

A mixed filter comprised of dispersive and nondispersive elements is a further possibility. Thus the first few stages of the structure could be CdS with easily manageable thicknesses (2 mm, 1 mm, 0.5 mm) producing the narrow bandwidth and the required FoV without splitting and the final stages being a higher birefringence nondispersive material such as $LiNbO_3$ giving the required FSR again with easily manageable thicknesses. Such tradeoffs will be considered further with the discussion of the filter model in section 6.

3.4 Tuning

There are several reasons why it is necessary to tune the peak transmitting wavelength of the filter after construction. Firstly a small degree of tuning is required to follow drift in the laser wavelength as mentioned in section 2.1. Secondly, tuning will ease the tolerances required in finishing the crystal plates to the precise thicknesses required. With CdS, in particular, where the dispersion of the refractive indices is not accurately known, much trial and error in the fabrication would be necessary to produce plates of the exact order required. However the most important reason to provide tuning of the filter is to compensate for drifts in temperature which will affect the values of birefringence and hence shift the transmittance peak. This effect is particularly severe for $LiNbO_3$ which has a temperature variation in birefringence of 4.5 x 10^{-5} $°C^{-1}$ which translates to a shift in wavelength of 0.3 nm/°C. Active tuning of the filter to keep the transmittance peak centred on the laser line would ease the need to achieve tight control of laser wavelength, filter temperature and manufacturing tolerances.

Possible methods of tuning include mechanical (changing orientation of the birefringent plates), electronic (using the electrooptic effect on suitable materials) and temperature. However, it is considered that the most convenient method appears to be the use of liquid crystal variable retardation (LCVR) plates in the thicker stages to offset the error in birefringence of the crystal plates [8,9]. Large variations in retardance can be produced in liquid crystals with low voltages and they are available with the required 50 mm aperture and good transmittance (>95%). Moreover the effect on FoV is expected to be negligible because of the low thickness of the device (<10 μm). When a LCVR is in series with a birefringent element, the retardance of

the combination is given by

$$\gamma = \gamma_L + \gamma_B$$

where $\gamma_L = \Delta n_L d_L$ and $\gamma_B = \Delta n_B d_B$, Δn_L and d_L are the birefringence and thickness of the liquid crystal and Δn_B and d_B are for the birefringent element. The LCVR is low order with $\gamma_L \leq \lambda$ whereas the birefringent element is high order with $\gamma_B \sim 1000\lambda$. If it is required that sufficient tuning be available to shift the peak of the transmittance by one FSR then the variation in retardance of the LCVR, $\Delta\gamma_L$, needs to be equal to the wavelength λ. Considering the various stages of a Lyot filter, ideally all would need to be tuned, requiring a LCVR in each stage. If the thickest stage is tuned by an amount γ then subsequent stages must be tuned by $\gamma/2$, $\gamma/4$ ... $\gamma/2^{N-1}$. With the proposed six stage filter indications from modelling are that only the five most sensitive (thickest) stages will require tuning due to the large bandwidth (low order) of the thinnest stages. To achieve a retardance variation of 532 nm, requires a change in birefringence of 0.106 for a 5 micron thick cell. Liquid crystal cells with such characteristics are readily available.

4 COMPONENT DISCUSSION

4.1 The Secondary Filter

The spectral transmittance of the birefringent filter consists of a series of narrow peaks. A secondary filter is required to suppress all peaks other than at 532 nm. A multilayer dielectric stack of the form $(HL)^3\ H((HL)^2\ H)^7\ (LH)^3$ where L is a low refractive index material and H the high index material, has been found to give adequate spectral transmittance. This construction is used in conjunction with filter glasses BG-39 and GG-475 to provide cutoff below 450 nm and above 630 nm. The filter is centred around 532 nm. H is zinc sulphide and L is cryolite and each layer is a quarter wave thickness. The filter has a pass band width of 40Å. The position of the central peak changes by 0.25 nm/deg and since the multilayer is sandwiched between glass cover plates, this is adequate to ensure the ± 8.5° FoV for the total filter. The transmittance of the combination of secondary filter and filter glasses with anti-reflection coatings is 76%. Much of the transmittance loss of the secondary filter is due to the filter glasses. The possibility of replacing these with appropriate coatings on the other surfaces of the primary filter, particularly the polarisers, has been investigated. A four layer design has been chosen for the antireflection coatings on the polarisers to give maximum transmittance at 532 nm. The effect of 12 of these 4 layer coatings, one on each side of each polariser, is not sufficient to fully suppress the sidebands of the secondary filter. Hence elimination of the filter glass is not feasible with this approach. Applying more complex coatings on the polarising stages introduces heat to the cemented elements which may result in breakdown of the bonding agent. Complex coatings applied to other elements such as the lithium niobate introduce a risk of delaminaton with the temperature extremes the filter is expected to experience.

4.2 Liquid Crystal Variable Retarder device control

An electronic controller for control of multiple LCVR's has been developed involving the use of one PC based 24 bit digital output card and an 8 channel control circuit. The control circuit [10], consists of multiplying 16 bit D/A converters and a 2 kHz driver. A single channel version of the circuit has been in operation for several months and operates satisfactorily. Three 8 channel devices are currently under construction.

4.3 Polarisers

The overall operation of the filter is very dependent on the performance of the polarisers between each stage. In particular, high transmittance of the pass polarisation and good rejection of the orthogonal polarisation is required to achieve the filter specifications on transmittance and sideband rejection. The desired properties of a polariser for this application are as follows: high transmittance and good extinction, preferably >90% and >100:1; 50 mm aperture; a thickness of approximately 4 mm and; FoV of > 10°. Two different approaches have been tried to achieve this specification on the polarisers.

4.3.1 Bleaching of commercially available polaroid sheet

Typical commercial sheet polariser, such as Polaroid HN-38, has a transmittance of approximately 76%. A bleaching process has been reported [11], which can increase this to above 90%. The bleaching process involves the use of temperature and humidity to remove the iodine from the film. Several attempts have been made with various combinations of temperature, humidity and exposure time. None of these attempts have been successful to date. However, other steps, (stripping, glass sandwiching and antireflection coating), involved in converting the commercial product to a suitable form for use in the filter have been successfully developed. Stripping involves chemical removal of the CAB protective coating to produce material for use in the bleaching process. Glass covering of the bleached film is required to protect the polarising film from further bleaching due to atmospheric conditions. The sandwiching process has been successful on stripped polaroid film. Antireflection coating on the glass covering reduces the reflection losses at the air/glass interface. For the sandwiched polaroid material the transmittance increases from 76% to 82%. A commercial product using higher transmittance HN-42 has been ordered for further assessment of this style of polariser.

4.3.2 Beam splitter polariser

An alternate approach for a suitable polariser has been considered [12]. It consists of an array of beam splitting polarisers (bsp), such as given in Figure 2a, which has the transmittance and extinction characteristics of a bsp but in a form giving a 50 mm aperture and thickness of 4 mm. A multiple element bsp has been constructed with a normal incidence transmittance of 92.5%, and greater than 100:1 extinction, 50 mm aperture and 4 mm thickness.

The transmission property of the polariser is determined by a combination of the performance of the dielectric coating and the obscuring effect of the joiner layer. The multiple glued joiner layers act as a 2.6% obscuration at normal incidence. The transmission function for the plane of maximum obscuration for a single polariser can be approximated by :

$$T = 0.95 \times \left(0.974 - \frac{t}{d} - \frac{x}{d} \tan\left[\sin^{-1}\left(\frac{\sin \gamma}{n}\right)\right]\right)$$

where γ is the incident angle in the obscuration plane, t is the thickness of the obscuration layer, x is the thickness of the polariser, d is the distance between obscuring layers and n is the refractive index of the prism material. The factor 0.95 is due to the efficiency of the dielectric coating between the bsp halves. This function is valid for light incident over the entire aperture. However, polarisers of this type have a limited field of view when used in series. A variation on the design using only half the number of obscuring layers, Figure 2b, improves the field of view as shown in Figure 3a. Figure 3b compares the predicted and measured transmittance as a function of angle for single and multiple polarisers. Modelling of the performance of multiple polarisers in the context of the proposed filter has shown the average transmittance of each polariser over all incoming angles to be 91.5%.

4.4 Filter Housing

A housing has been constructed, Figure 4, for the purpose of multiple component testing and as an aid in consideration of mounting problems associated with each element. The housing allows the following functions to be performed : testing of the active control system for up to three stages of the LADS filter; measurement of field of view properties in azimuth and elevation; and study of temperature effects on the filter performance. Features of the housing include: 360° rotation about centre axis; closely spaced elements; windows on outer sides for improved temperature stability; temperature control through water flow or heater tape; capability for measurement of rotational angle to 1°; ±5° alignment of components; access to the individual elements for removal with no effect on the alignment of other components; and external connection to pairs of liquid crystal control wires.

4.5 The Liquid Crystal Variable Retarder

A liquid crystal variable retarder (LCVR) was obtained from Meadowlark Optics Inc., having an active layer of E44 material (maximum birefringence 0.26) which was 3.35μm thick. With glass cover plates and antireflection coatings the transmittance at 532 nm was 95%. The cell has a clear aperture of 50 mm and a thickness of 13 mm. A major concern was the lack of uniformity of the retardance over the area of the aperture. By placing the cell between crossed polarisers and rotating its optic axis 45°

to the polariser pass plane, the retardance of the cell may be varied by adjusting the voltage applied to give an absolute minimum in transmittance corresponding to a retardance of an integer number of wavelengths of the light. With these settings of azimuth and voltage the variation in retardance across the cell may be examined. A typical result of the measurement of transmittance across the aperture is shown in Figure 5. The dark ring in this figure indicates the portion of the cell where a full wave retardance existed giving maximum extinction of transmitted light. By varying the voltage applied, this ring could be moved from the cell centre to the outer extremity and from a previously measured calibration curve of voltage versus retardance, the retardance variation was estimated to be 35±5 nm. Alternatively, with a constant voltage applied to the cell, the dark rings may be made to expand or contract by tilting the cell to vary the angle of incidence. Complete movement across the aperture is achieved with a tilt of 7°. Thickness variation alone cannot explain both of the measured results simultaneously (values of thickness difference between centre and edge of 0.44 μm and 0.0007 μm were obtain from the two methods). The methods could only be reconciled by assuming a difference in alignment of the optic axis of the liquid crystal between the centre and the outside edge of the cell of some 3°. The calculations necessary to arrive at these conclusions were conveniently made using the exact theory of [2].

Two additional liquid crystal cells have recently been obtained which are constructed with lower birefringence materials (1. #2140, Δn=0.125, d=5.19μm and 2. #2244, Δn=0.07, d=10.5 μm). Both cells are able to achieve the full tuning range required (max γ_L>532 nm) but have considerably better uniformity with measured retardance variations of ±1 nm. This is not surprising since it has been shown that a decrease in Δn results in improved retardance uniformity [13].

The effect of nonuniformity of these and other components can be modelled by assuming a retardance that varies linearly with distance from the centre of the cell and integrating the transmittance over the aperture. Results of total transmittance versus wavelength for a cell with a retardation variation of 35 nm show a small shift in peak position, no discernible change in bandwidth and a change in maximum (and minimum) transmittance from 100% (0%) to 99.3% (0.7%). The shift in peak position can be easily accommodated by tuning the LC. The changes in transmittance cause a minor degradation in the signal to noise. The effect of birefringence variation on the total filter performance has been further investigated and is discussed in section 6.

A further complication which arose with these cells was that of etaloning between the inside surfaces of the cell walls. Figure 6 is the transmittance versus voltage characteristics of the E44 cell, with the polariser and analyser absent, and the optic axis at zero volts and parallel to the polarisation of the input beam. The modulation is due to the refractive index changing with voltage and the etalon going through its maxima and minima. There is no doubt that the etaloning is due to reflections from the inside surfaces since, when this device was placed in a spectrometer, fringes were observed which had a free spectral range corresponding to the thickness of the cell. The reason this etaloning was being observed was due to the very high degree of parallelism achieved in these particular cells. In other studies of poorer cells etaloning was not observed because the degree of nonparallelism "washed out" the fringes. Figure 6 also contains transmittance versus voltage characteristics with the analyser

absent but with the optic axis at 45° to the input polarisation. The fringes are still present, however the modulation depth is decreased due to the fact that the interfering rays are no longer of the same polarisation. For completeness the transmittance versus voltage characteristic with the optic axis perpendicular to the input polarisation is included. In this case no modulation is observed due to the fact that with the optic axis in this orientation the radiation picks up zero change in refractive index. Unfortunately there is no convenient way to eliminate these etaloning effects.

4.6 The Lithium Niobate Crystal Material

Four slices of lithium niobate ($LiNbO_3$) crystal were obtained from Crystal Technology Inc. (CTI). These were 3 mm thick and 50 mm in diameter and were oriented as 'y-cut' which means that the optic axis was in the plane of the slice and as such the slices were birefringent for light travelling through the large faces. One slice was polished by Applied Physics Division of CSIRO using their teflon polishing procedure and techniques developed previously for $LiNbO_3$ for tunable Fabry-Perot etalons [7]. The flatness achieved was better than $\lambda/40$ with faces parallel to 10 seconds of arc. The thickness of this slice was measured by mechanical methods as 2786 μm, with the accuracy $\pm$ 1 μm sufficient to establish the order to $\pm$1 using the known birefringence of 0.09. CSIRO also developed a method of measuring birefringence by monitoring transmittance of collimated laser light (at λ= 544 nm), and tilting to give a curve of transmittance versus tilt angle [14]. The angular separation between two minima in this curve gives the birefringence and the measurements agreed well with the published value. In-house measurements of birefringence of the slice using a different technique incorporating an optical multichannel analyser (OMA) and a white light source initially did not give agreement with published data. This discrepancy has since been resolved and was due to the affect of the dispersion of the birefringence on the spectral transmission function. This technique involved measuring the spectral transmittance of the slice between parallel polarisers which is the arrangement of a single stage birefringent filter with trasmittance described by the first two equations of section 3.1. Analysis of the measurements gives the detailed spectral variation of the birefringence and promises to be a satisfactory method for measuring this quantity in materials of interest for birefringent filters.

The variation in retardance across the slice face was measured by placing the slice between crossed polarisers and oriented with optic axis at 45°, and using the LCVR to provide a variable retardation. By adjusting the voltage on the LCVR a minimum in transmitted intensity of the combination for 532 nm light could be achieved. However the transmitted light showed variation across the aperture as typified by Figure 7. This variation differed to that of the LCVR as discussed in section 4.5, showing bands of constant retardation rather than the radial variation of the LCVR. The bands were perpendicular to the optic axis which was the crystal growth direction, suggesting some variation of growth conditions with time. The retardance variation across the slice was measured by varying the voltage on the LCVR and moving the band of minimum intensity across the slice.

The variation in birefringence was determined to be 2 x 10^{-5} /mm. Negotiations with the material supplier, CTI, have succeeding in having them grow a crystal specifically for lower birefringence variation and indications are that future material could have a variation of less than 10^{-7} /mm. One sample piece of such material has been obtained and has been assessed. This piece was polished by CSIRO and examined by us as described above. There were two distinct regions, divided by a line perpendicular to the optic axis. Extinction could be obtained separately in both but with a measured retardance difference between the two regions of 60 nm. Within each region the retardance variation was less than 20 nm which corresponds to a birefringence variation of 5 x 10^{-6}/mm suggesting high quality material of the required size is definitely possible.

The modelling that was done with the LCVR was modified to describe the banded variation seen with the $LiNbO_3$, and similar results were obtained. For a variation in retardance of 70 nm across the aperture as measured, there was no change in bandwidth of the transmittance versus wavelength response but there was a small decrease in the modulation depth and a shift in peak position. As with the LCVR, the effect of the decrease in modulation depth on the SNR was included in the modelling for the total filter structure in section 6.

4.7 Cadmium Sulphide Crystal Material

A sample piece of cadmium sulphide CdS was obtained from Cleveland Crystals Inc. Although 50 mm aperture material is available, it is very expensive and a smaller piece, 20 x 20 x 2 mm, was obtained to assess optical quality and to develop polishing techniques. The slice was polished by CSIRO using their teflon polishing technique with very good results similar to that obtained with the lithium niobate. The optical quality was also very good, and although this piece was z-cut (optic axis perpendicular to large face) it was possible to assess the birefringence variation across the slice by tilting. This appeared to be considerably better than that of the $LiNbO_3$ or LCVR, however a quantitative measurement was not made. An additional piece of y-cut CdS, acquired some years ago by CSIRO, was also polished with no differences in working for the different cuts being encountered. With this piece of material it was possible to verify the wide field aspects of this material and a sample stage of the filter comprising polarisers, LCVR and CdS slice was assembled. The wide field properties were essentially verified and tuning via the LCVR was also demonstrated.

However a major concern with CdS was the absorption at 532 nm. Antireflection coatings were applied to both sides of the slice and the transmittance measured at 532 nm for the 2 mm path length was 70%. This loss was judged as unacceptably high for the LADS application when combined with the other losses (principally from the polarisers) in a total filter structure.

4.8 Half wave plate

Half wave plates are required in each of the split element, wide field stages when $LiNbO_3$ is used as the birefringent material. The requirement on these elements are

that they give a half wave retardance at 532 nm and across the full FSR of the filter, ± 4 nm. A zero order ($\Delta n\ d = \lambda/2$) half wave plate made from a single piece of lithium niobate or quartz meets this requirement but would require a thickness (d=28μm for quartz) which is impractical over a 50 mm aperture. A technique of using two pieces of birefringent material oriented at 90° to each other and having thicknesses differing by $\lambda/2$, has the same broadband features. Such an element made from quartz was obtained from CVI. Although it was nominally centred at 532 nm it was actually centred at 570 nm when measured between parallel polarisers with a white light source and the OMA. The performance at 532 nm, although within the CVI specification, was slightly degraded (transmittance of 6% instead of zero). However, the resulting degradation of performance of a single stage of the filter at normal incidence was minimal. Again, the chief effect was a degradation of the modulation and hence the SNR. CVI have indicated that future components supplied would be more accurately centred at 532 nm.

Modelling (section 6) of the complete filter with a compound zero order half wave plate indicates there would be a reduction in performance by approximately 16% compared to a true zero order half wave plate. This reduction is due to the decreased field of view of the compound half wave plate. At incident angles other than normal, the transmittance is dependent on the total thickness of the half wave plate and the azimuth angle [15]. A true zero order half wave plate constructed by sandwiching a polymer material between glass is available from Meadowlark Optics Inc. and has been selected as a replacement for the compound plate. No experimental assessment has yet been done of this component.

5 EXPERIMENTAL ASSESSMENT OF A COMPLETE STAGE

Full testing of tunable filters requires investigation of several different aspects of performance. These are:

1) measurement of the spectral transmittance including central wavelength, bandpass and free spectral range ;
2) measurement of the maximum transmittance and sideband rejection ;
3) measurement of the field of view characteristics ;
4) assessment of the uniformity of transmittance across an aperture ;
5) assessment of the change of the filter characteristics to temperature which is particularly important for this filter with its lithium niobate elements;
6) speed of response of the tuning to external changes.

Ideally each component of each stage should be individually tested, followed by each stage, leading onto a gradual build up and testing of the full device. The results of testing of individual components has been described in section 4.

In order to carry out the full testing as described above an experimental arrangement was designed and assembled which allowed investigation of the filter at the central wavelength of 532 nm and recording of the spectral transmittance using a white light source. Figure 8 is a diagram of the experimental setup. An optical multichannel analyser (OMA) and white light source were used to record the spectral transmittance of the filter. The white light source was

expanded and collimated using a standard lens system and an iris placed in the beam allowed illumination of varying aperture sizes. The OMA was calibrated using three different laser lines, 514 nm, 532 nm and 544 nm. The transmittance measurements were carried out using a cw, doubled YAG laser which was chopped, expanded to a diameter of 35 mm and thereafter brought to normal incidence on the filter. The radiation from all sources ultimately followed the same path onto the filter entrance and at that point was normal to the planes containing the optic axes of the birefringent elements. Lens L1 collected all of the light and focussed it onto the signal detector, D2. Detector D1 monitored the reference signal. Both detectors were large area silicon photodiodes and the outputs from both detectors were fed into lock-in amplifiers. Outputs from the amplifiers were read directly into a personal computer.

The ability to illuminate varying aperture sizes of the filter with monochromatic light allows a very rapid assessment of the uniformity of birefringent components This may be done either visually by observing fringes or by measuring the contrast ratio as a function of aperture size - a decrease in contrast ratio would indicate nonuniformities. A more accurate assessment of an element may be carried out using a small-spot size laser beam and "mapping" the surface by measuring any change in voltage required to achieve the same contrast ratio as the central portion. Note that measurement of contrast ratio is a much more sensitive indicator of nonuniformities than measurement of the maximum transmittance value.

5.1 Field of view of a single stage

The field of view for a complete single stage has been measured for wide and non wide field cases. The arrangement of elements for these stages is shown in Figure 9. For the wide field case the polarisers were aligned such that their pass planes were at 0° in azimuth. The two lithium niobate elements of the same thickness, (2786 μm) with the optic axis of the first lithium niobate element rotated 45° to the polariser pass planes, were seperated by a compound half wave plate with its optic axis parallel to the polariser pass plane. The second lithium niobate was oriented with its optic axis at 90° to that of the first piece. For the non wide field case the half wave plate was removed and the second piece of lithium niobate was rotated by 90° such that the optic axes of the two pieces were parallel. For both wide and non wide field cases, the liquid crystal retarder axis was parallel to the optic axis of the first lithium niobate. The entire stage could be rotated in azimuth about the centre axis by using the housing described in section 4.4.

Measurements were made at a number of azimuth angles and the results are shown in Figures 10, 11 and 12. The measured transmittance matches closely to the prediction using a numerical model. If the half wave plate was a true zero order half wave plate there would be no change in transmittance with azimuth angle. Figure 13 shows the predicted transmittance for a true zero order half wave plate and Figure 14 shows this for the compound half wave plate. The reasons for the small discrepancies between measurement and theory are due to slight misalignment of some of the components in the experiment.

5.2 Spectral transmittance

The measurements of the spectral transmittance of the wide field stage using the OMA gave expected results for the bandpass of 0.3 nm. Maximum transmittance for the full aperture at 532 nm was measured as 24% which is close to the estimate of 25.5% obtained by compounding the transmittances of individual components, (low transmittance polarisers were used for this test). Minimum transmittance at 532 nm was measured, by appropriately tuning the LCVR, as 1.2%, however this will be considerably reduced by the addition of the further stages in the complete filter.

6 MODEL OF FILTER

A numerical model has been developed to evaluate the cumulative effects of imperfections in individual components on the transmittance of the total filter. A uniform illumination of the entrance aperture of the receiver telescope is assumed as is a uniform angular distribution within a solid angle of 20 mrad. The telescope optics transform this angular distribution to that shown in Figure 15 at the first polariser. The integration necessary to assess the effect of variations in the individual filter components across the aperture is carried out by first performing a ray trace through the filter structure for different starting positions and directions, applying the effect of every component on each ray, and summing the results with weighting determined by the intensity and angular distributions at the first polariser. The effect of the individual components is determined using a modified Jones matrix method rather than the exact treatment described in [2] to reduce computation time. The usual Jones method assumes no reflections from surfaces and does not allow for angles of incidence away from normal. However all surfaces in the filter are to be antireflection coated and, due to the thickness of the components, etalon effects will be on a scale much smaller than the filter bandwidth and can be neglected. The effect of the non-normal incident angles can be included by using the known variation of refractive index with angle in the birefringent elements and appropriately adjusting the path length. Comparison of the results of this model for some sample ray paths with the exact calculations of [2] and an extended Jones matrix method due to Yeh [16], have been made and no significant differences have been observed for cases relevant to this filter construction.

The variation across the aperture of the individual components is modelled as described in section 4 where the variation in birefringence is proportional to position and thickness for the lithium niobate elements and proportional to the radius for the LCVR's. The overall effect is quantified as a figure of merit, (FoM), defined as the ratio of the integrated transmittance (over angle, area and wavelength) which is within the laser bandwidth to the total integrated transmittance outside the laser bandwidth.

6.1 Figure of merit as a function of element thickness

Changing the thickness of the lithium niobate elements alters the FoM as indicated by Figure 16. Increasing the thickness of the elements reduces the bandwidth of the central peak and the FSR. The FoM increases until the sideband peaks and residual ripple become more significant than the reduction in noise due to the reducing bandwidth of the central peak. The sideband peaks are caused by a differential shift

of the wide field and non wide field elements at non normal incident angles.

6.2 Number of filter stages

The effect of increasing the number of stages in the filter is indicated in Figure 17. The FoM improves due to the reduction of bandwidth and residual ripple. The transmittance of the filter reduces due to the extra components, particularly the additional polarisers. The specification of 25% minimum transmittance for the filter restricts the number of stages to 6.

6.3 Effect of birefringence error on figure of merit

Measurements of the liquid crystal and lithium niobate have shown that variations in birefringence occur in each of these components. The source and measurement of this error is discussed in more detail in sections 4.5 and 4.6. The effect of the birefringence errors on FoM is indicated in Figure 18. Figure 18 compares the FoM for 5 and 6 stage filters, with and without the measured birefringence error. The experimentally observed value of birefringence variation would give approximately 9% reduction in FoM.

6.4 Comparison of number of wide field elements

The two types of element, wide field and non wide field have a small difference in spectral shift with incident angle. When a non wide field element is modelled, integration of the incident light over all relevant incident angles results in a small sideband peak. A wide field element does not show this peak. The second and more important effect of using a wide field element is the improvement in FoM due to the field of view response at a constant wavelength. Figure 19 compares 5 and 6 element filters as a function of the number of wide field elements and element thickness. If the thickness of the thinnest element in the filter is 0.3 mm, there is no advantage in using a wide field element in the thinnest stage. However, if the thinnest element is 0.7 mm, the FoM is improved significantly by having the thinnest stage as a wide field stage.

6.5 FoM as a function of secondary filter bandwidth

Reducing the secondary filter bandwidth allows the free spectral range of the birefringent filter to be reduced. For the same number of stages this also results in a reduced bandwidth and a greater FoM. Figure 20 compares the predicted FoM for filters constructed with 5 and 6 stages using secondary filters with a bandwidth of 4nm and 8 nm. There is a significant improvement in FoM for a filter with a 4 nm filter compared to an 8 nm secondary filter. The element thickness at which maximum FoM occurs is determined by the secondary filter bandwidth.

6.6 Other factors

The model also allows for inclusion of the effects of partial polarisation and thickness errors for the half wave plate and lithium niobate. The effects of these type of imperfections ' small compared to the effect of the birefringence variation for the lithium niobate and LCVR.

7 ACTIVE TUNING OF THE LYOT FILTER STAGE

7.1 Single stage tuning

Temperature changes within the filter assembly produce a change in the filter transmittance due to the changing birefringence and thickness of each lithium niobate element. Compensation for these changes is necessary to maintain maximum throughput of the laser wavelength and continued suppression of other wavelengths. We have demonstrated active tuning with a LCVR, using a simple iterative method based on a steepest ascent gradient algorithm. This has been shown to be an appropriate method of control for the single stage of the LADS filter [17]. The algorithm has been modelled and shown to be suitable for the control of a multiple stage filter. The algorithm is in two parts. The first achieves a good approximation to the best opeating voltage. The second part, discussed here is appropriate to the tracking or maintenance of control voltage due to temperature change.

A typical filter transmittance versus applied voltage characteristic, T(v), for the combination of liquid crystal and lithium niobate is shown in Figure 21. In this figure the operating voltage required is shown at A. The following algorithm is used to change the operating voltage from an arbitrary voltage v_n to a better solution v_{n+1}, where v_{n+1} is closer to A.

repeat :

$$\delta v = g(v_n)$$

$$\xi_n = T\left(v_n + \frac{\delta v}{2}\right) - T\left(v_n - \frac{\delta v}{2}\right)$$

$$\Psi = \frac{\left|\sum_{k=n-p}^{n} \xi_k\right|}{p}$$

$$\beta = K + M(v_n) \times \Psi$$

$$\Delta v = \beta \times \xi_n$$

$$v_{n+1} = v_n + \Delta v$$

: *loop*

where:

- δv = sample interval, dependant on the current operating voltage;
- $g(v)$ = sample interval function formulated such that samples are seperated by equal changes in retardance;
- $T(v)$ = filter transmittance as a function of voltage;
- ξ_n = difference in transmittance over the sample interval;
- v_n = current operating point;
- v_{n+1} = new operating point;
- K = fixed multiplier term;
- M = additional multiplier term inversely proportional to the slope of the retardance curve;
- Ψ = absolute value of average slope calculated over the last p samples;
- Δv = correction to operating point;
- p = number of samples required for averaging.

Samples of the transmittance of the filter are taken at voltages determined by the sample interval function g(v). This function has been evaluated experimentally by measurements of the retardance characteristics of the liquid crystal. The correction made to the operating point is dependent on the sign and magnitude of the transmittance difference at the two sample voltages. The additional factor $M\Psi$ is used to improve the multiplier β in situations where insufficient correction is made in the iteration process. The $M\Psi$ value increases if the average transmittance error increases. The values for K and M can be optimised to increase the rate at which the operating voltage is achieved. The range of values for K and M which produce a stable iteration are determined experimentally. M is approximately inversely proportional to the slope of the retardance versus voltage curve.

In operation, the system will be correcting for continuous drifts in temperature. Rapid temperature changes will produce conditions where the adjustment to the operating voltage is not sufficient to achieve an adequate correction. This is due to the changing characteristic of the transmittance function T(v) with temperature, Figure 22. For a multiple stage system there is a similar equilibrium condition which will occur at a lower rate of temperature change.

The performance of the tuning algorithm for a single wide field stage of the filter has been evaluated. The experimental arrangement used the wide field and non wide field elements described in section 5.1 mounted in the housing (section 4.4) and surrounded by heater tape to provide the temperature changes. Figure 23 compares the tuned and untuned transmittance for a temperature change of approximately 5°C over 20 min. The tuned transmittance remains close to the maximum over the entire period of the experiment whereas the untuned transmittance changes rapidly as the temperature of the lithium niobate changes. There are small changes (<3%) in the tuned transmittance caused by etalon interference in the liquid crystal with the precise magnitude of the etalon effect dependant on the control voltage used on the LCVR. The cause of the etalon interference is discussed in more detail in section 4.5.

The results presented in Figure 23 were obtained with an aperture of 5 mm whereas Figure 24 compares the performance of the filter using the tuning algorithm for two apertures of 5 and 30 mm. There is a significant reduction in the tuned transmittance dependent on the temperature gradient across the lithium niobate which causes a birefringence gradient across the element. The temperature gradient across the lithium niobate was estimated from measurements from a pair of thermocouples glued to a glass substrate situated close to the lithium niobate element where the thermal properties of the glass substrate are representative of those for the lithium niobate.

7.2 Multiple stage tuning

Temperature changes in each filter stage produce changes in retardance proportional to the thickness of the lithium niobate elements in the stage as discussed in section 3.4. This, together with the nonlinearity of the compensating LCVR's retardance with voltage and the possibility of temperature gradients along the length of the filter, result in a need for separate control of each LCVR device. No compensation is

thought achievable for the temperature gradients across the elements and this is neglected in the following discussion.

The tuning algorithm for the single stage was extended for the multiple stage filter by tuning individual stages in a specified sequence. The algorithm selects the next filterstage to be adjusted when the magnitude of the change in transmittance achieved through iteration is below a user defined value or if a predefined maximum number of iterations have been performed.

A numerical model has been developed to allow an evaluation of the tuning algorithm when used in a multiple stage filter. The model has been used to find the maximum rate of change of temperature that can be compensated. This limit is dependent on the response time of the liquid crystal and the sample frequency. Several laser pulses are sampled to eliminate the pulse to pulse variations in intensity of the laser. In the evaluation of performance an arbitrary failure level of 80% of the static performance of the algorithm has been assumed.

Figure 25 indicates the predicted average performance of the control algorithm when used for a five stage filter. The filter is subject to a continuous temperature change for a test period of 18 min. The performance limit or maximum rate of temperature change that the algorithm can correct, has been recorded as a function of the time delay between samples. The effect of the interference caused by the etalon in each LCVR is also included in Table 3.

Table 3. Effect of Interference Caused by Etalon

sample interval	no etalon	etalon
100 msec	1.4 °C/min	1.1 °C/min
400 msec	0.5 °C/min	0.4 °C/min

The etalon interference effect can reduce the total transmittance by 20% for the static case. The effect also reduces the allowable rate of temperature change by approximately 20%.

The sequence in which the filters stages are tuned has been selected as 1,2,3,4,5 where the thickness of the stages is $1<2<..<5$. Modelling of an alternate sequence whereby the filter associated with the thickest lithium niobate element is adjusted most frequently eg : 5,4,2,5,3,5,4,5,2,3,5,4,5,1, has not shown any improvement in the average performance of the filter for simple thermal situations.

8 SUMMARY

A birefringent filter of the Lyot design could considerably enhance the ability of the LADS system to detect laser light in the presence of ambient sunlight. Numerical modelling has determined quantitatively the amount of improvement and indicated the optimum design to consist of six stages giving a bandwidth of 0.1 nm and free spectral range of 7 nm to be used in conjunction with a dielectric filter of effective bandwidth 7 nm . The total filter should have a field of view of ± 8.5° and transmittance greater than 30% to give an improvement by a factor of 20 in figure of merit over the currently used filter. Several options for the components of the filter have been evaluated both theoretically and experimentally. As a result lithium niobate is recommended as the main birefringent material and this choice necessitates the use of active tuning of at least five stages to compensate for variation in birefringence due to temperature fluctuations. Tuning via liquid crystal variable retarders has been successfully demonstrated along with the ability to 'track', in an automatic fashion, laboratory and deliberately induced temperature variations. In addition it becomes necessary to use wide field element construction incorporating zero order half wave plates in at least five stages to achieve the required field of view. Measurements of field of view of a single stage pointed to the need for a zero order rather than a compound half wave plate and a commercial supplier of suitable devices has been identified. The overall transmittance of the filter is critically dependant on the transmittance of the polarisers and a novel design with greater than 92% transmittance has been successfully fabricated. A commercial supplier of an alternate cheaper polariser has also been located, (however this has not yet been assessed). An experimental housing has been developed which has design concepts suitable for use in the full filter. Electronic hardware and control software for the tuning of a single stage are also suitable for extension for use in a complete filter.

9 RECOMMENDATIONS

On the basis of the success of the assessments described in this report it is recommended that construction of a complete filter proceed. The housing and control system should be designed for a six stage filter with each stage incorporating a liquid crystal variable retarder and a wide field element. The suggested structure is illustrated in Figure 26. Progressive testing during assembly of the complete filter will be required to determine the optimum number of stages and the number requiring active tuning and wide field design.

10 ACKNOWLEDGMENTS

It is a pleasure to acknowledge the encouragement and support of members of the LADS team, Mike Penny, Ralph Abbot and Allan Hicks, throughout the course of this work. Much helpful advice and support has come from John Venning, Alex Hope, Mick Levin, Graham Fowler, Derek Verringer, Geoff Burls and Allan Britton. We have also greatly benefited from collaboration with CSIRO Division of Applied Physics and with Chris Walsh, Achim Leistner and Zoltan Hegedus in particular.

REFERENCES

1. Lyot B., "Birefringent Filters", Ann. Astrophys., 7(1-2), 31-35, 1944
2. Seymour R.S. and Staromlynska J. "Computations using an exact 4×4 matrix method for the optics of anisotropic media", in preparation.
3. RCA Electro-optics Handbook, p70, Fig 6.9.
4. Yeh P., "Dispersive birefringent filters", Optics Comm., 37(3), 153-158, 1981.
5. Evans J.W., "The Birefringent filter", J.Opt.Soc.Am. 39(3), 229-242, 1949.
6. Title A.M. and Rosenberg W.J., "Tunable birefringent filters", Opt.Eng., 20(6), 815-823, 1981.
7. Burton C.H., Leistner A.J. and Rust D.M. "Electrooptic Fabry-Perot filter: development for the study of solar oscillations", Appl. Optics, 26(13), 2637-2642, 1987.
8. Kaye W.I., "Liquid crystal tuned birefringent filter", U.S. Patent 4394 069, July 19, 1983
9. Staromlynska J., "Electro-optic broadband tunable filters using liquid crystals", J. Mod. Optics, 37(4), 639-652, 1990
10. Burnard P., private communication.
11. Gunning W.J. and Foschaar J. "Improvement in the transmittance of Iodine-polyvinyl alcohol polarisers" Appl. Optics, 22(20), 3229-3231, 1983.
12. Richards J. and Rees S., "Efficient large aperture polariser", Prov. patent.
13. Staromlynska J., "A double element liquid crystal tunable filter - factors affecting contrast ratio", IEEE JQE, 28(2), 501-506, 1992.
14. Hegedus Z., private communication.
15. Hale P.D. and Day G.W., "Stability of birefringent linear retarders (waveplates)", Applied Optics, 27(24), 5146-5153, 1988
16. Yeh P., "Extended Jones matrix method", J.Opt.Soc.Am., 72(4), 507-513, 1982.
17. Seymour R.S., Rees S., Staromlynska J., Richards J. and Wilson P. "Design considerations for a liquid crystal tuned Lyot filter for laser bathymetry", submitted to Optical Engineering, 1993.

THIS PAGE BLANK

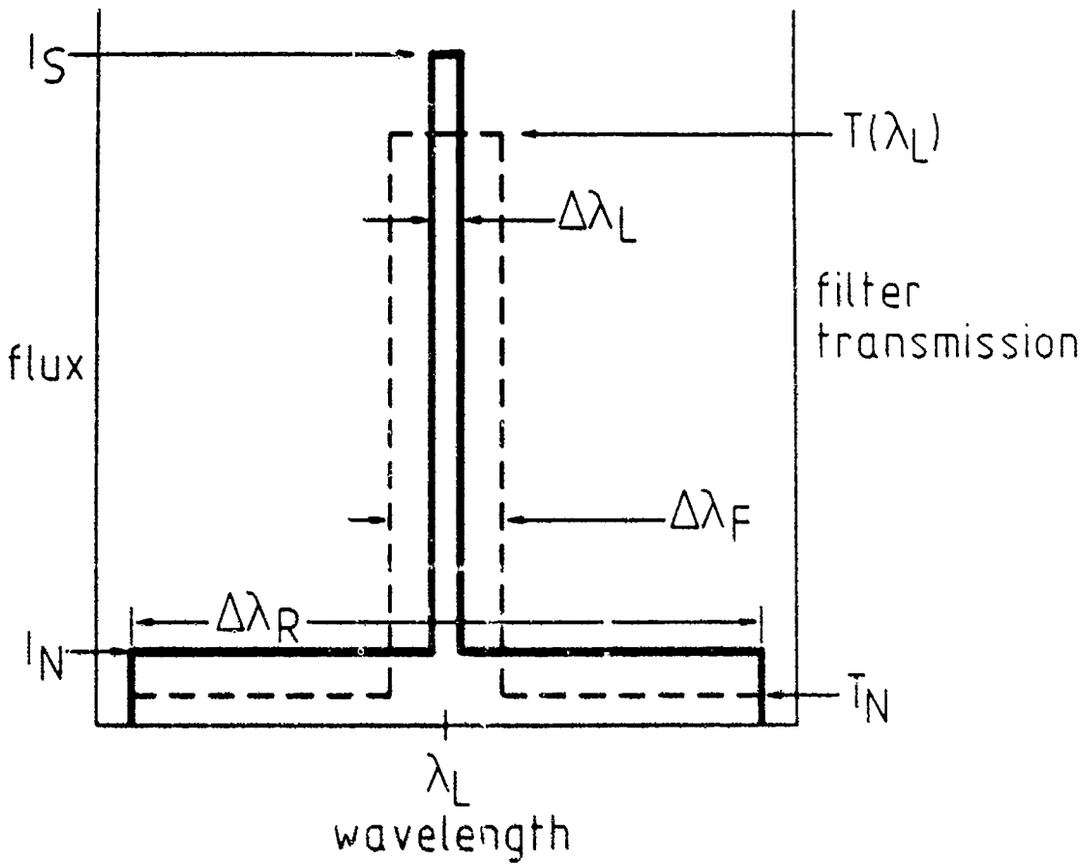

Figure 1. Idealised input light flux (solid) and filter transmittance (dashed) as a function of wavelength.

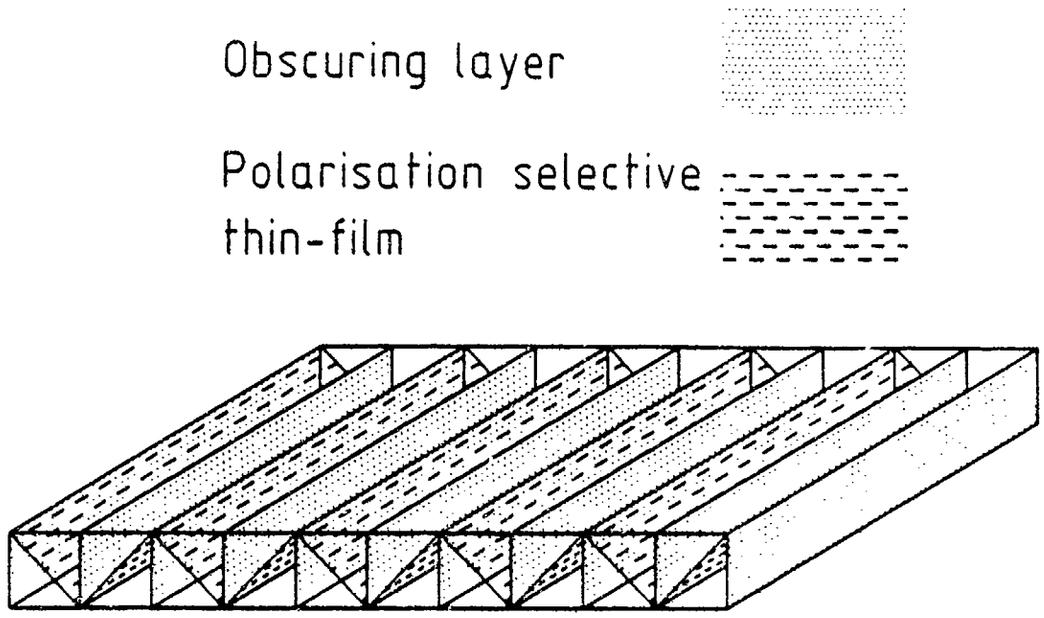

Figure 2a. Schematic diagram : Beam splitter polariser type 1

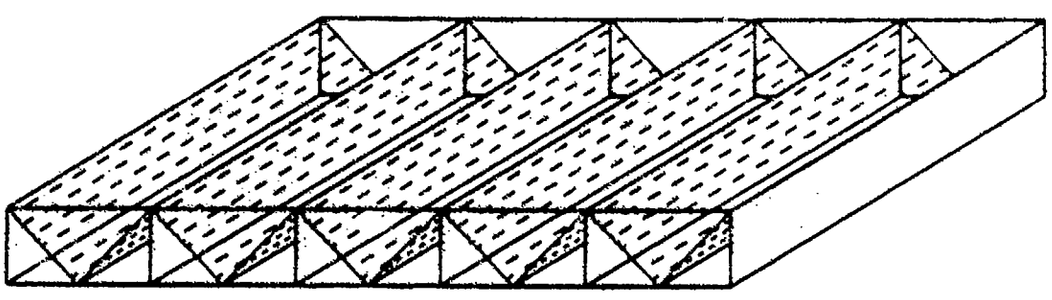

Figure 2b. Schematic diagram : Beam splitter polariser type 2

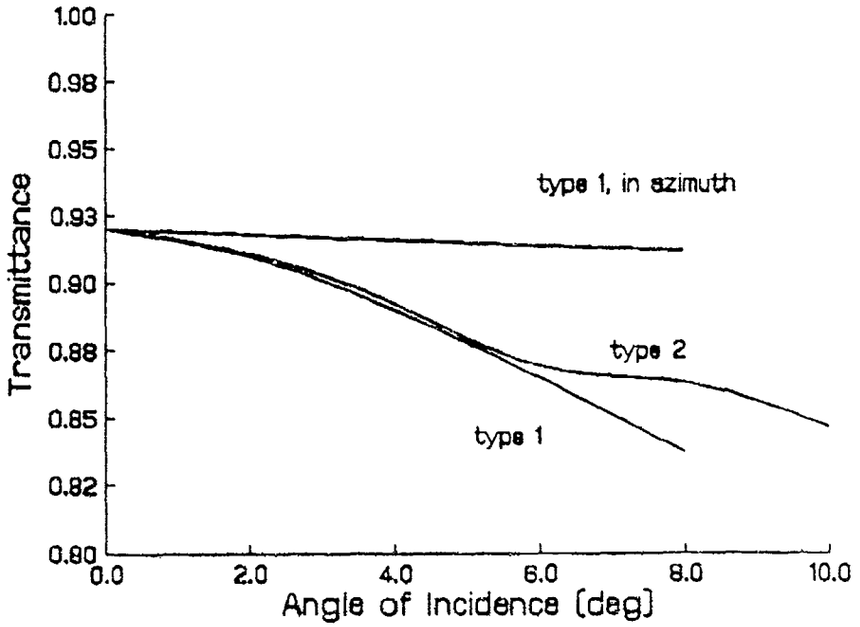

Figure 3a. Measurements showing field of view for type 1 and 2 polarisers

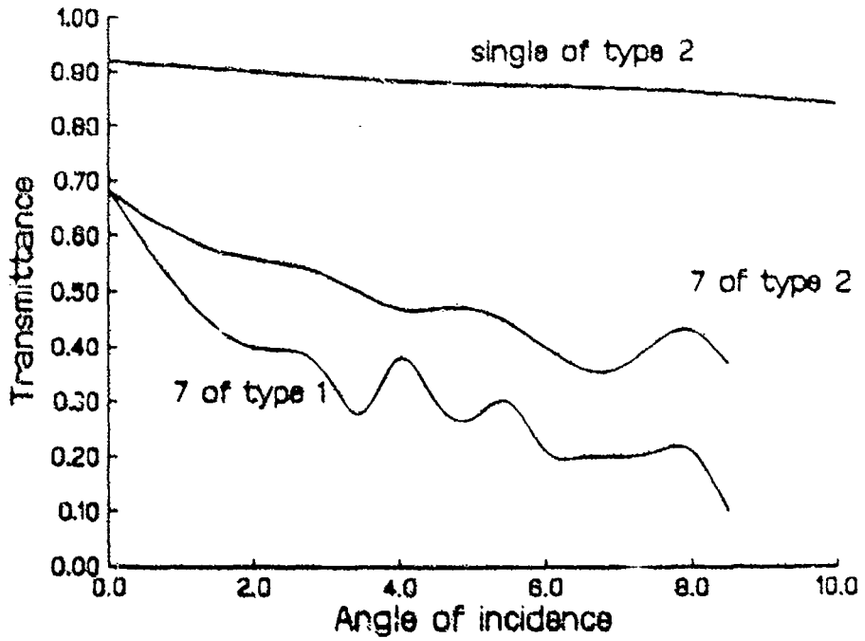

Figure 3b. Prediction showing field of view for single and multiple polarisers

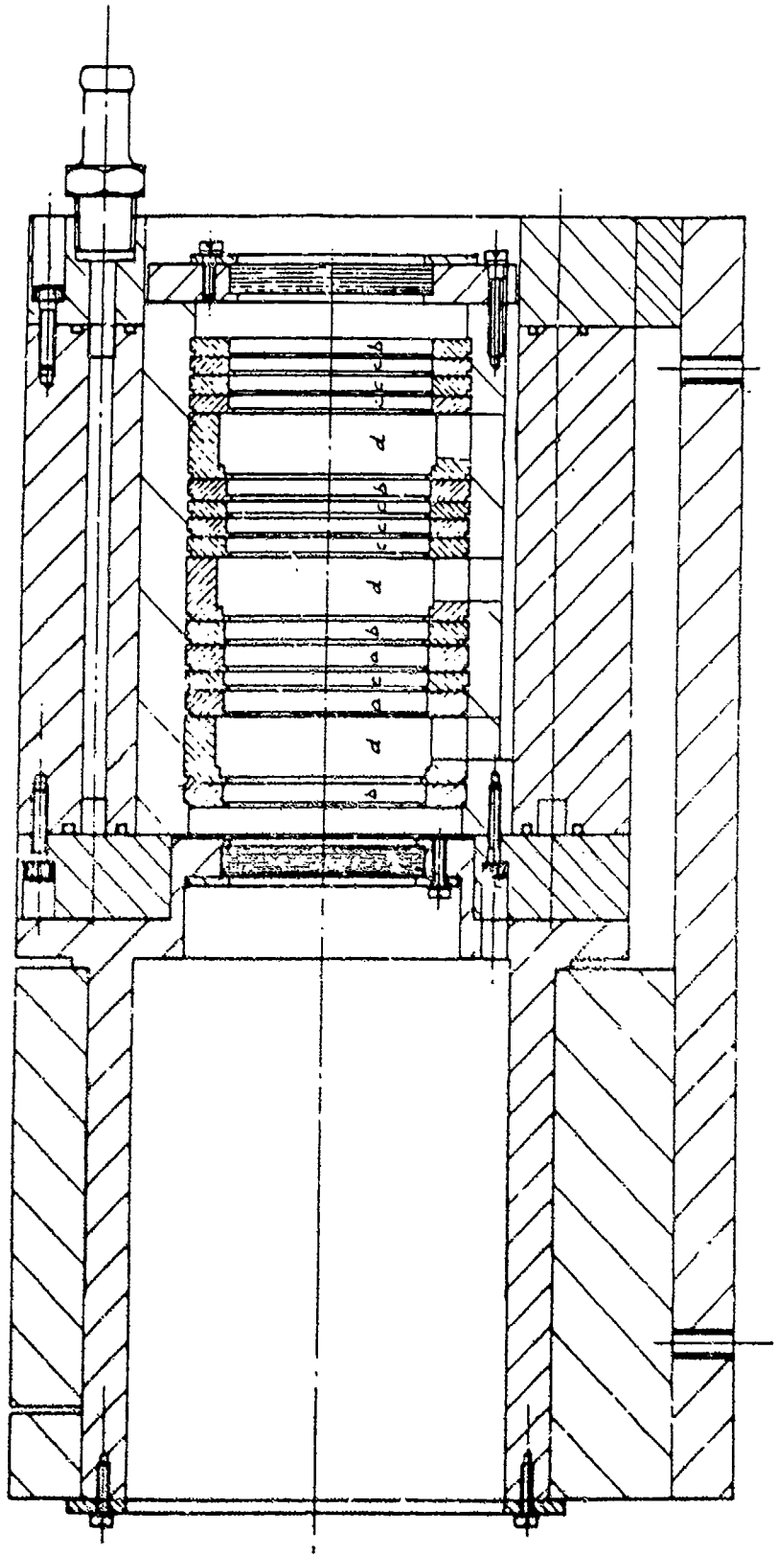

Figure 4. Housing for test bench

Figure 5. Birefringence variation for LCVR type E44

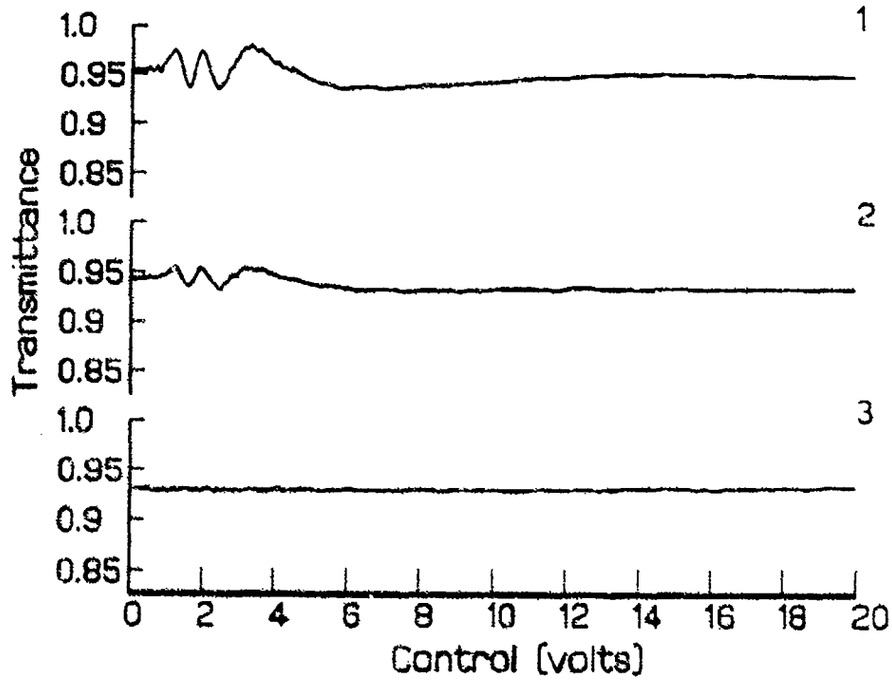

Figure 6. Etalon interference effect in liquid crystal retarder

Figure 7. Birefringence variation for lithium niobate

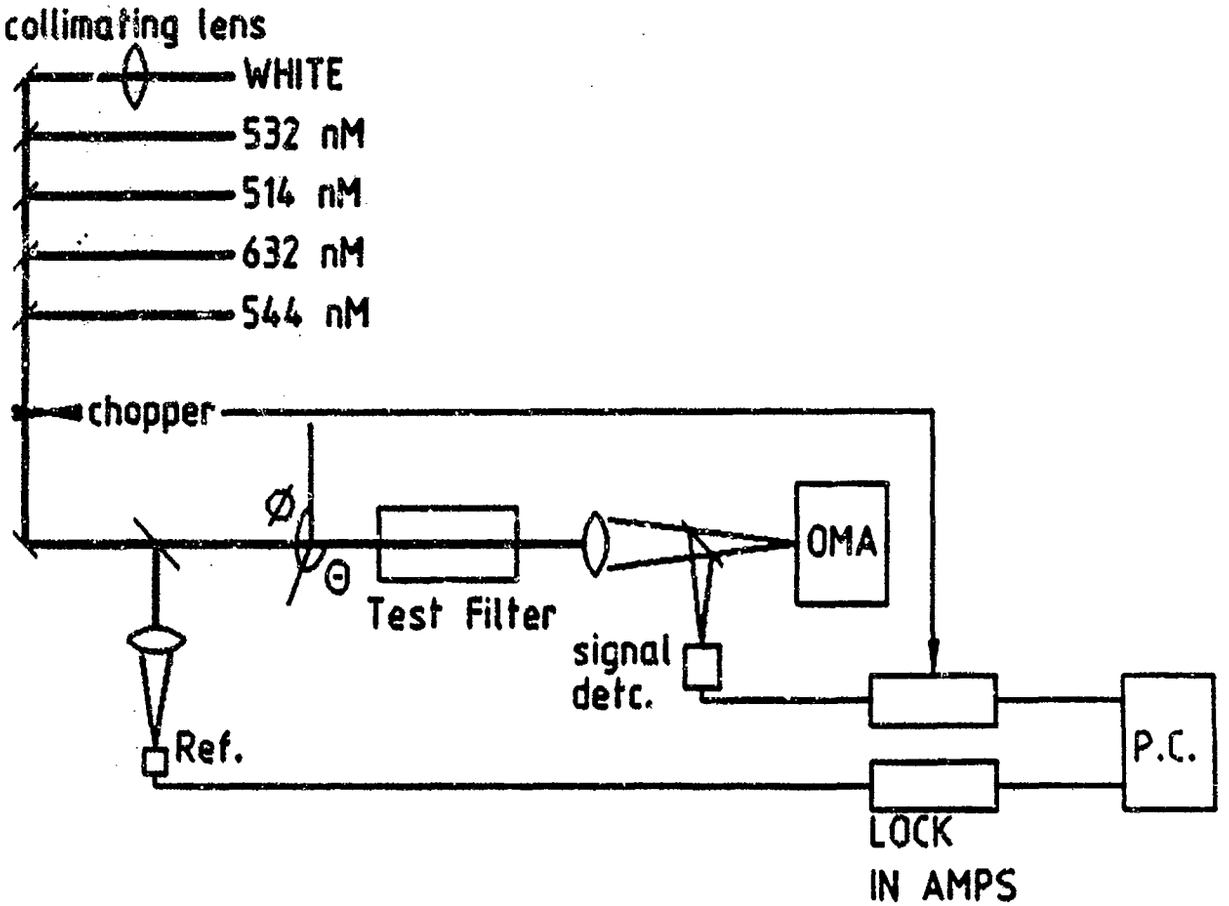

Figure 8. Experimental arrangement

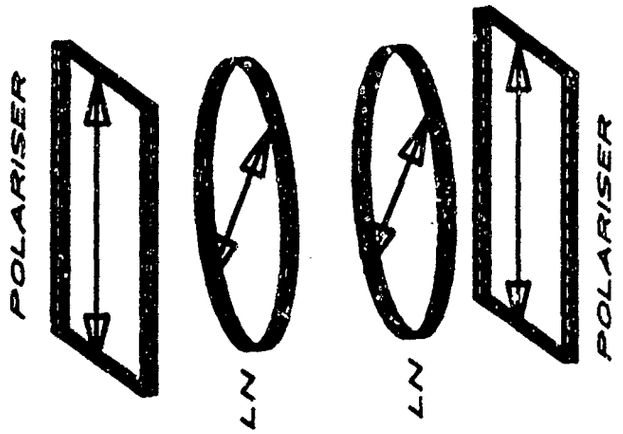

Simulated non wide field element

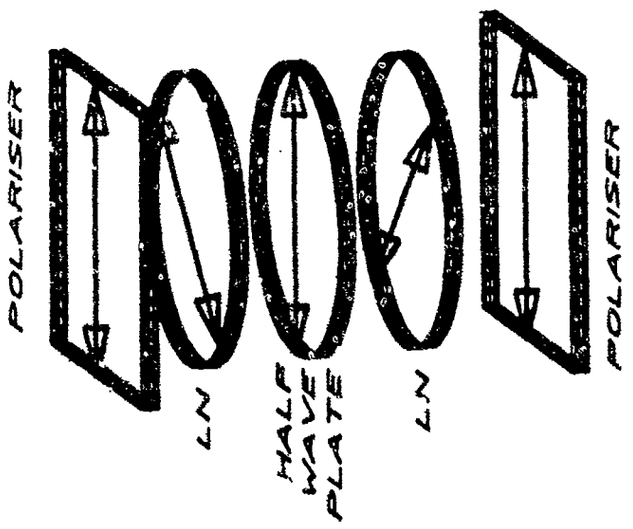

Wide field element

Figure 9. Construction of stage

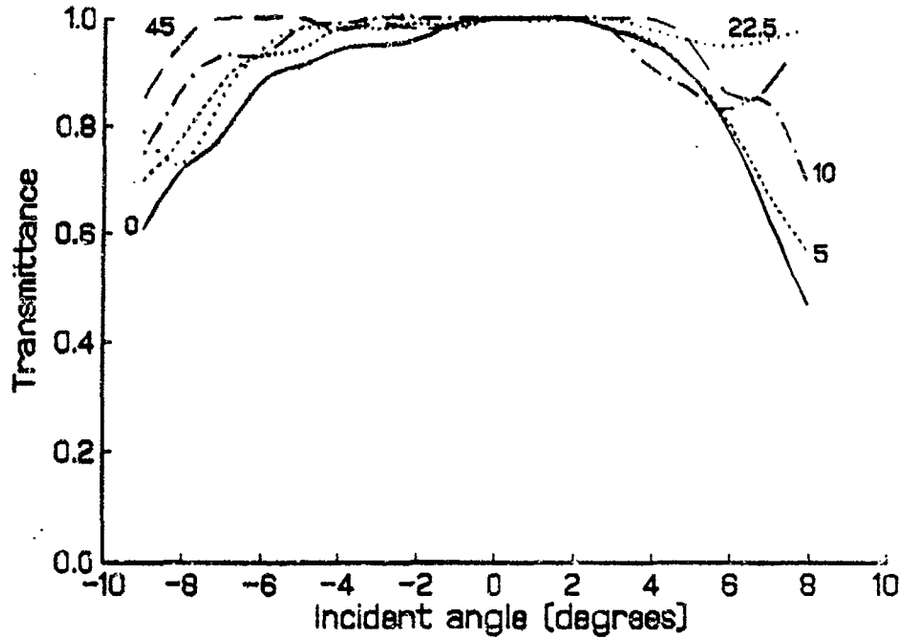

Figure 10. Measurements showing field of view for wide field stage with a compound half wave plate

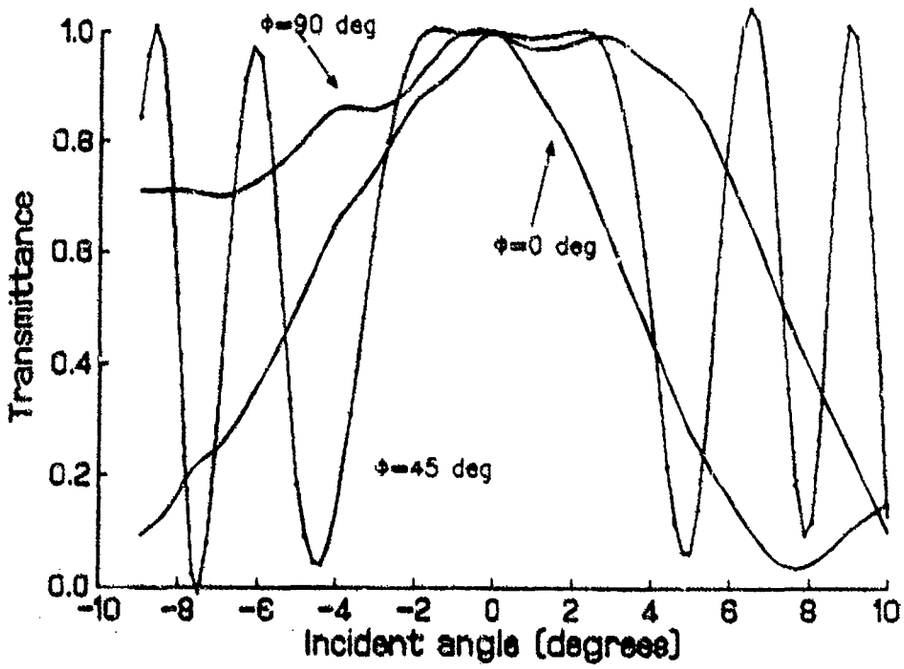

Figure 11. Measurement showing field of view for a non wide field stage

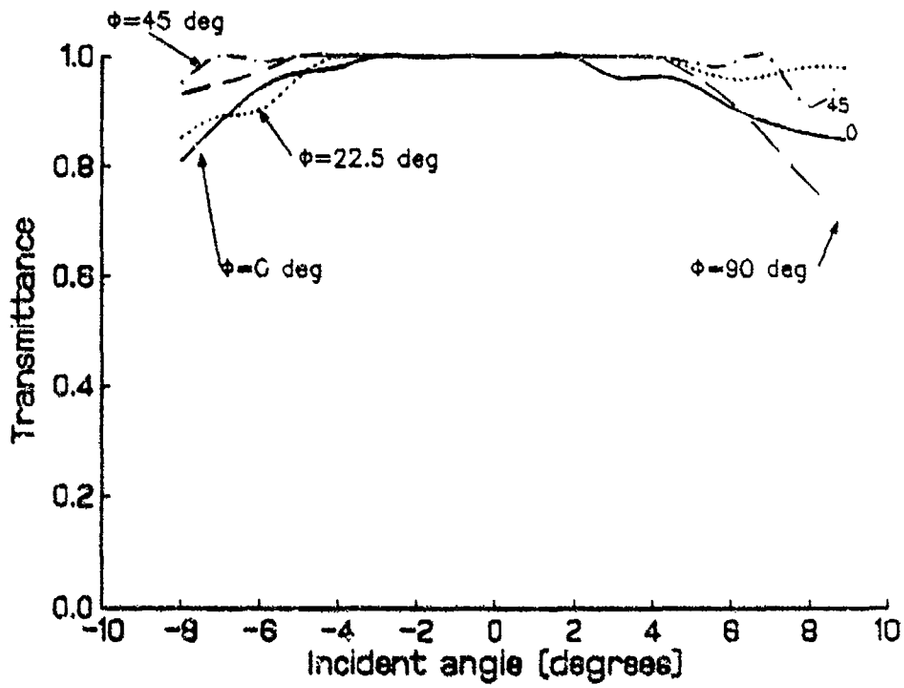

Figure 12. Measurement showing field of view for a wide field stage with a zero order half wave plate

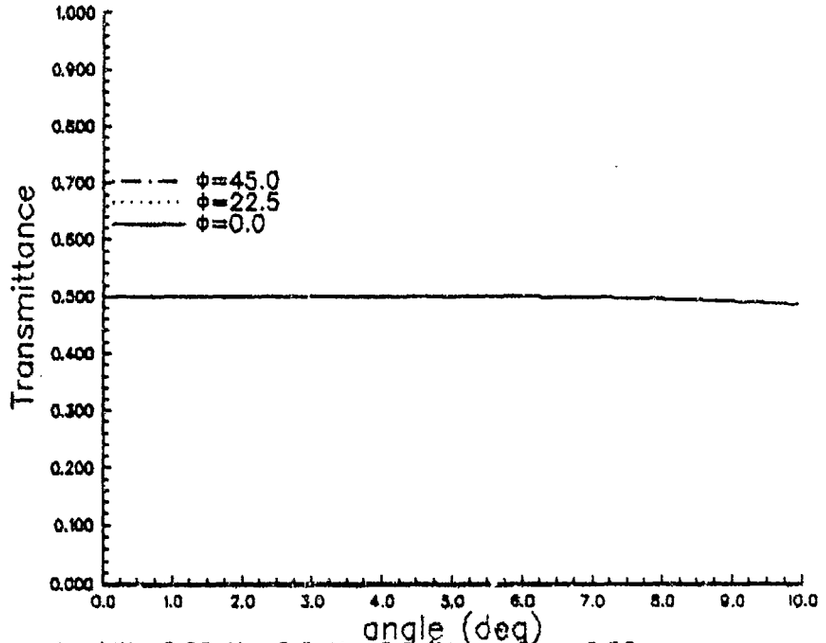

Figure 13. Prediction showing field of view for a wide field stage with a zero order half wave plate

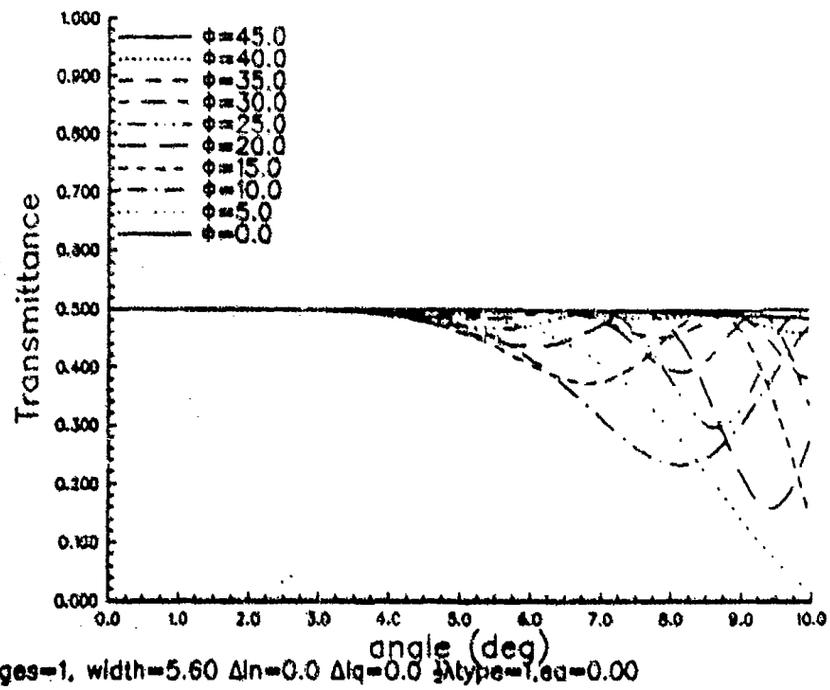

Figure 14. Prediction showing field of view for a wide field stage with a compound half wave plate

Figure 15. Population of incident rays at the focal plane as a function of angle

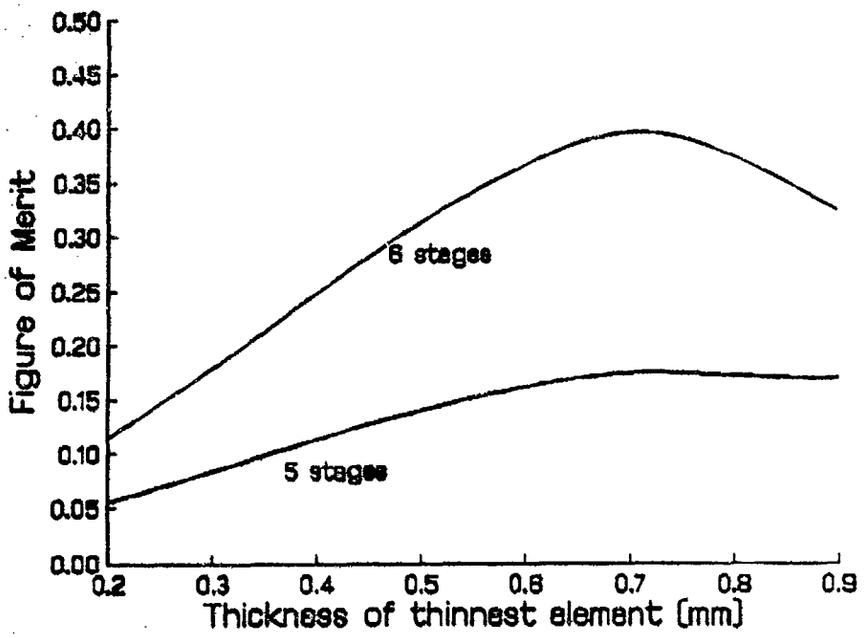

Figure 16. Figure of merit as a function of thickness of thinnest stage

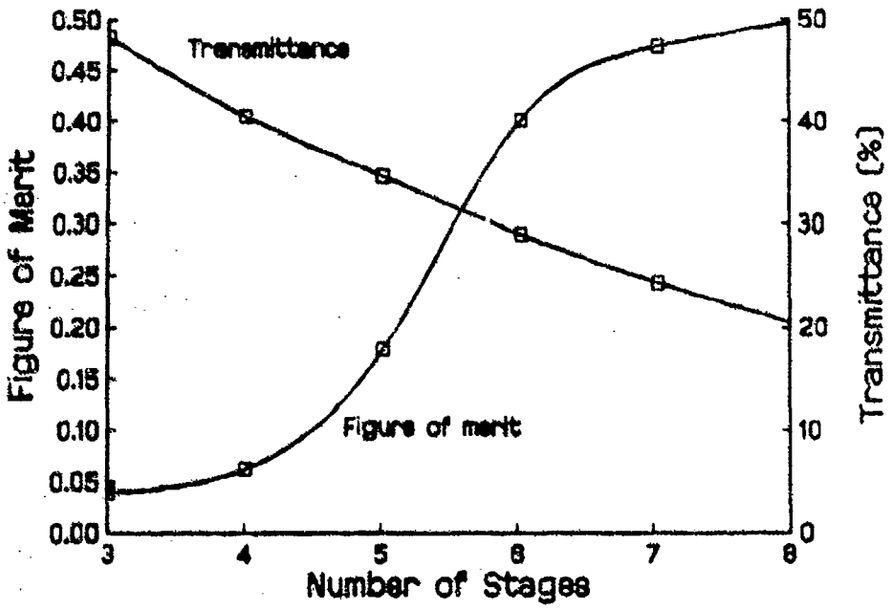

Figure 17. Transmittance and figure of merit as a function of number of stages

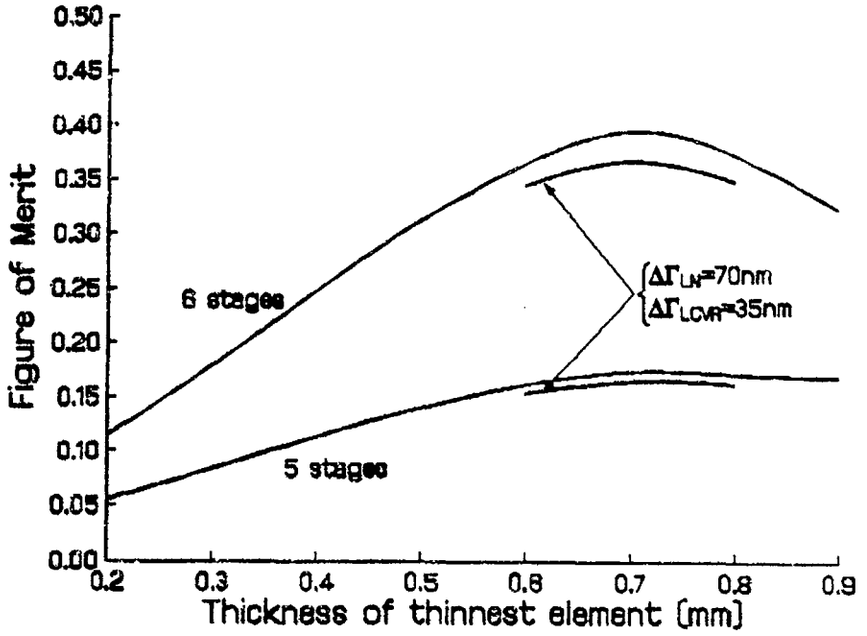

Figure 18. Effect of birefringence error on figure of merit

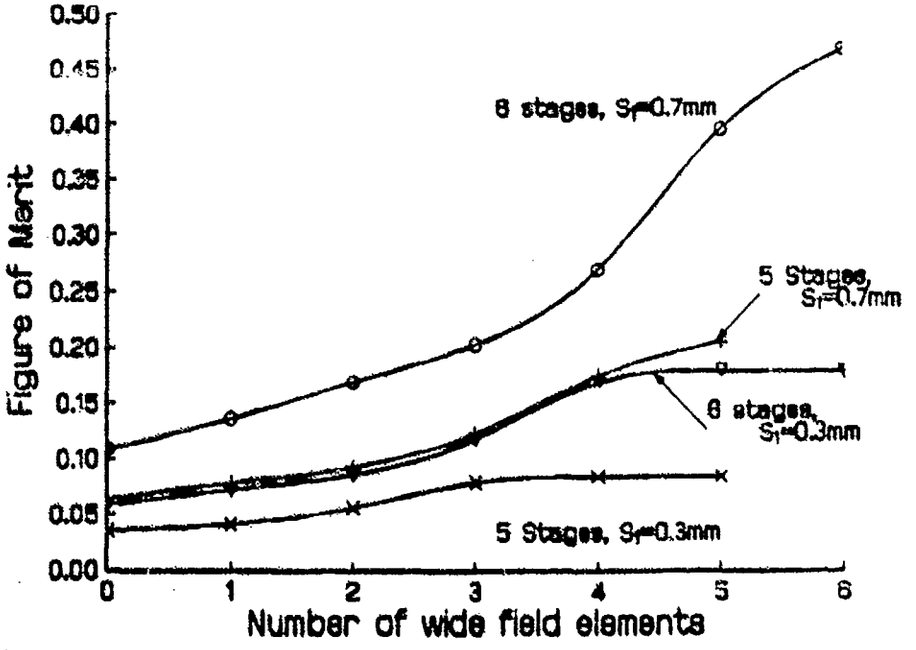

Figure 19. Figure of merit as a function of number of wide field elements

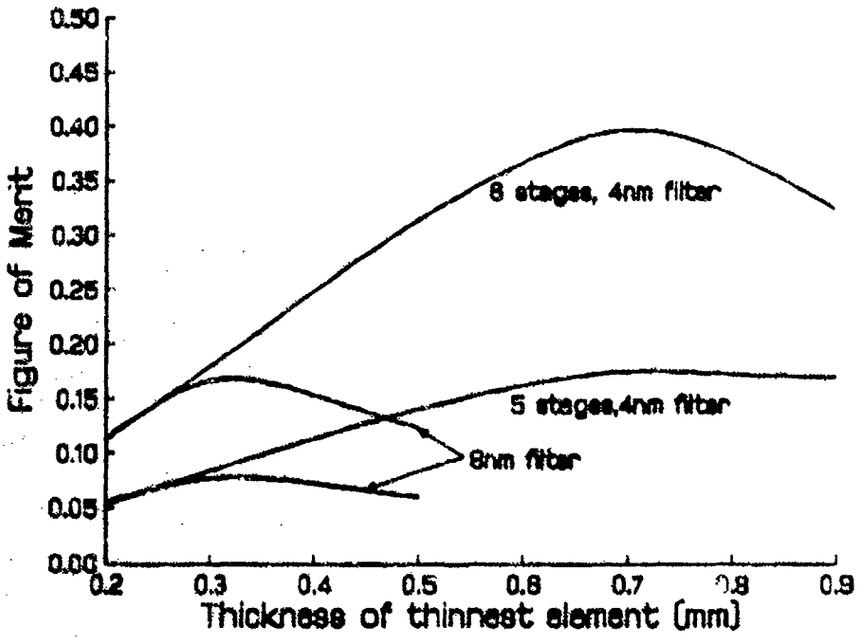

Figure 20. Effect of secondary filter on figure of merit

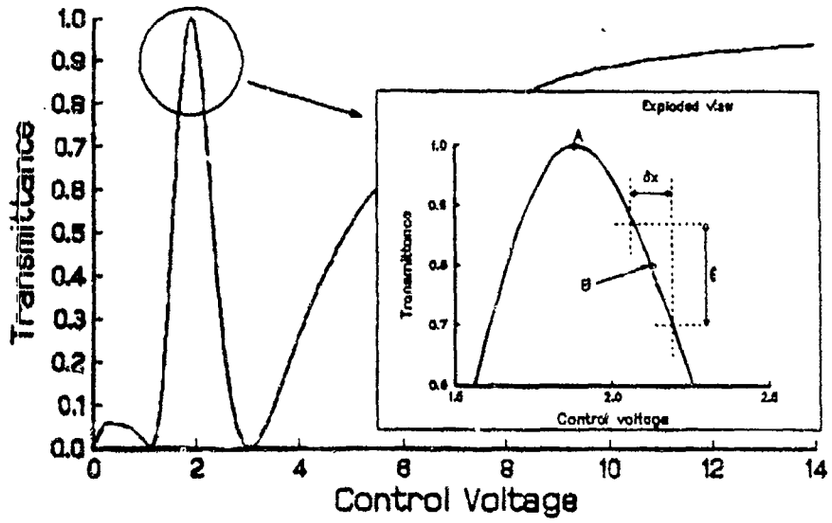

Figure 21. Transmittance-voltage characteristics for typical LCVR

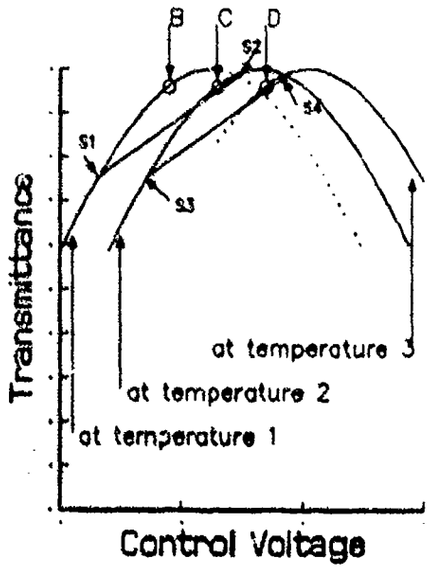

Figure 22. Correction to operating point for single stage

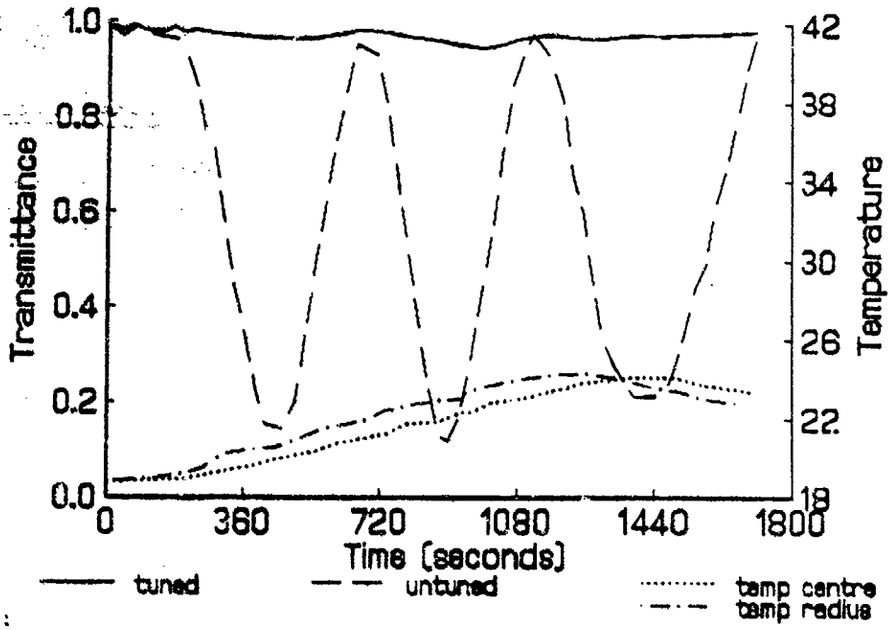

Figure 23. Comparison between tuned and untuned response to a constant rate of temperature change for a wide field element (small aperture)

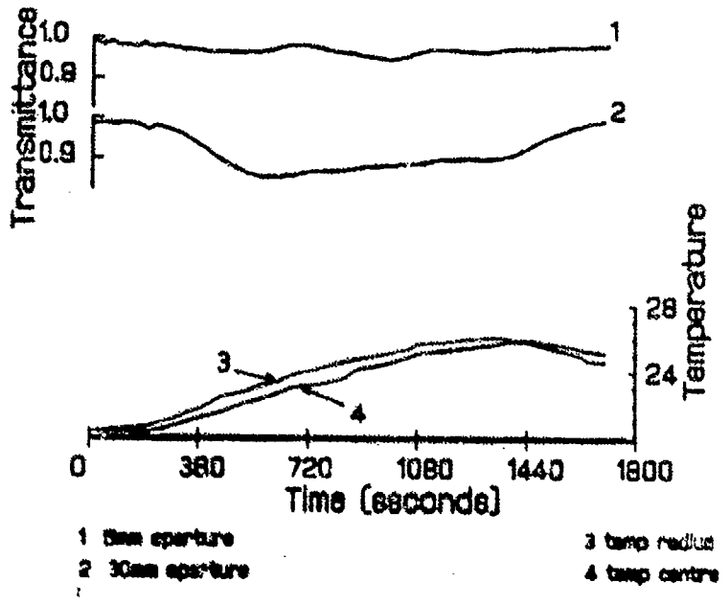

Figure 24. Comparison of tuned transmittance to a temperature gradient for small and large apertures

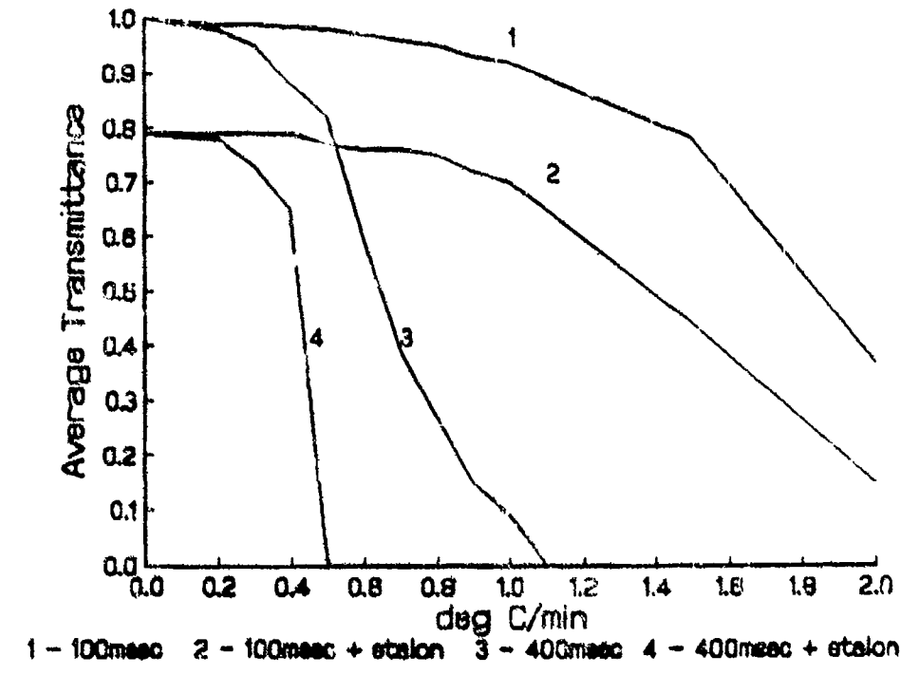

Figure 25. Performance of tuning algorithm with 100 and 400 msec delays between samples

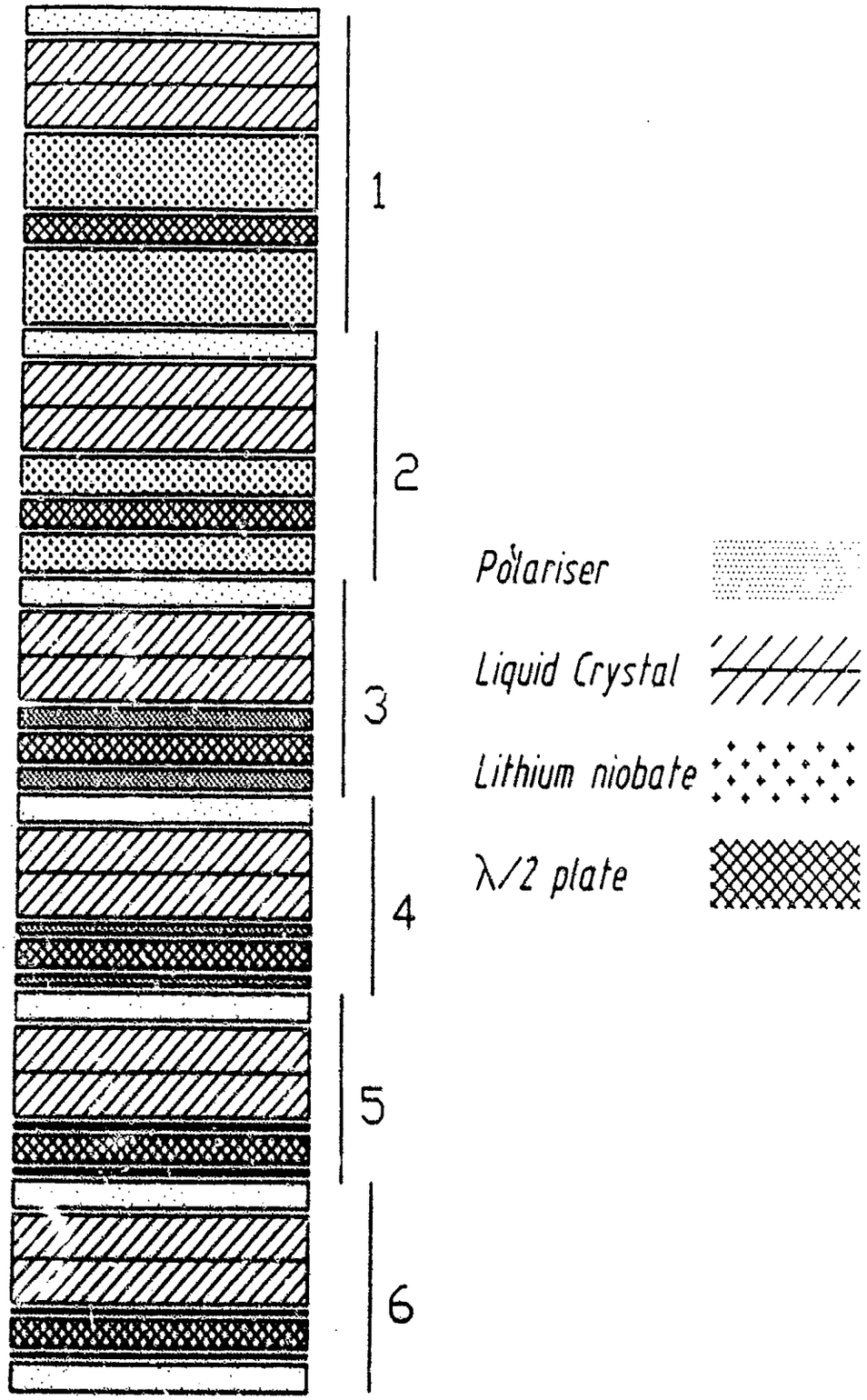

Figure 26. Proposed structure of complete filter

DISTRIBUTION

	Copy No.
CSIRO	
Dr C. Walsh, Applied Physics Division, NML	1
Defence Science and Technology Organisation	
Chief Defence Scientist)	
Central Office Executive)	1 shared copy
Counsellor, Defence Science, London	Cont Sht
Counsellor, Defence Science, Washington	Cont Sht
Scientific Adviser, Defence Central	1
Navy Office	
Navy Scientific Adviser	1
Navy Hydrographer	1
Air Office	
Air Force Scientific Adviser	1
Army Office	
Scientific Adviser, Army	1
Defence Intelligence Organisation	
Scientific Adviser, Defence Intelligence Organisation	1
Surveillance Research Laboratory	
Director	1
Chief, Optoelectronics Division	1
Research Leader, Surveillance Devices	1
Research Leader, Surveillance Systems	1
Research Leader, Optoelectronics Systems	1
Manager, LADS	1
LADS Project Director	1
Head, Optoelectronics Technology and Trials	1
R.S Seymour (Author)	1
S. Rees (Sub Author)	1
J. Staromlynska (Sub Author)	1
J. Richards (Sub Author)	1
P. Wilson (Sub Author)	1
R. Abbot, LADS	1
J. Venning, OETT	1
G. Fowler, ACS	1
M. Levin, OP	1
Media Services	1
Electronics Research Laboratory	
Chief, Electronic Warfare Division	1
M. Brown, ISP	1
Chief, Communications Division	1
Research Leader, Communications Countermeasures	1

Libraries and Information Services

Australian Government Publishing Service	1
Defence Central Library, Technical Reports Centre	1
Manager, Document Exchange Centre, (for retention)	1
National Technical Information Service, United States	2
Defence Research Information Centre, United Kingdom	2
Director Scientific Information Services, Canada	1
Ministry of Defence, New Zealand	1
National Library of Australia	1
Australian Defence Force Academy	1
Defence Science and Technology Organisation Salisbury, Research Library	2
Library Aeronautical Research Laboratories	1
Library Materials Research Laboratories	1
Library Defence Signals Directorate, Melbourne	1
British Library Document Supply Centre	1

Spares

Defence Science and Technology Organisation Salisbury, Research Library	6

Department of Defence

DOCUMENT CONTROL DATA SHEET

Page Classification	
UNCLASSIFIED	
Privacy Marking/Caveat (of Document)	
N/A	

1a. AR Number	1b. Establishment Number	2. Document Date	3. Task Number
AR-008-107	SRL-0109-TR	Nov 92	NAV 91/463

4. Title

EVALUATION OF A SINGLE STAGE OF THE LADS FILTER

5. Security Classification

Document	Title	Abstract
U	U	U

S (Secret) C (Confi) R (Rest) U (Unclass)

* For UNCLASSIFIED docs with a secondary distribution LIMITATION, use (L) in document box.

6. No. of Pages	54
7. No. of Refs.	17

8. Author(s)

R.S. Seymour, S. Rees, J. Staromlynska, J. Richards and P. Wilson

9. Downgrading/Delimiting Instructions

N/A

10a. Corporate Author and Address

Surveillance Research Laboratory
PO Box 1500
SALISBURY SA 5108

10b. Task Sponsor

NAV

11. Officer/Position responsible for

Security..... SOSRL

Downgrading..... DSRL

Approval for Release..... DSRL

12. Secondary Distribution of this Document

APPROVED FOR PUBLIC RELEASE

Any enquiries outside stated limitations should be referred through DSTIC, Defence Information Services, Department of Defence, Anzac Park West, Canberra, ACT 2600.

13a. Deliberate Announcement

No limitation

13b. Casual Announcement (for citation in other documents)

[√] No Limitation

[ ] Ref. by Author , Doc No. and date only.

14. DEETEST Descriptors

Laser Airborne Depth Sounder, Filters, Signal to noise ratio, Daylight, Performance evaluation

15. DISCAT Subject Codes

1709

16. Abstract

A tunable, large aperture, wide angle, narrowband filter, centred at 532 nm, has been developed to improve the signal to noise in the Laser Airborne Depth Sounder. Several new concepts have been included in the design.

Page Classification
UNCLASSIFIED

16. Abstract (CONT.)

17. Imprint

Surveillance Research Laboratory
PO Box 1500
SALISBURY SA 5108

18. Document Series and Number	19. Cost Code	20. Type of Report and Period Covered
SRL-0109-TR	802990	TECHNICAL REPORT

21. Computer Programs Used

N/A

22. Establishment File Reference(s)

N/A

23. Additional information (if required)